AD-A181 455 FINITE-DIFFERENCE MODELING OF SEISMOLOGICAL PROBLEMS IN 1/1
MAGNITUDE ESTIMAT (U) TELEDYNE GEOTECH ALEXANDRIA VA
ALEXANDRIA LABS K L MCLAUGHLIN ET AL MAR 87
UNCLASSIFIED TGAL-87-01 AFGL-TR-87-0106 F19628-85-C-0035 F/G 17/10 NL

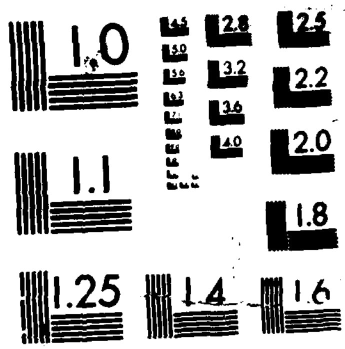

MICROCOPY RESOLUTION TEST CHART
NATIONAL BUREAU OF STANDARDS-1963-A

(12)

AD-A181 455

AFGL-TR-87-0106

FINITE-DIFFERENCE MODELING OF SEISMOLOGICAL PROBLEMS IN MAGNITUDE ESTIMATION USING BODY WAVES, SURFACE WAVES AND SEISMIC SOURCE IMAGING

Keith L. McLaughlin
Zoltan A. Der
Rong-Song Jih
Alison C. Lees
Lisa M. Anderson

Teledyne Geotech Alexandria Laboratories
314 Montgomery Street
Alexandria, VA 22314-1581

MARCH 1987

FINAL REPORT
11 February 1985 --- 10 February 1987

APPROVED FOR PUBLIC RELEASE; DISTRIBUTION UNLIMITED

AIR FORCE GEOPHYSICS LABORATORY
AIR FORCE SYSTEMS COMMAND
UNITED STATES AIR FORCE
HANSCOM AIR FORCE BASE, MASSACHUSETTS 01731

"This technical report has been reviewed and is approved for publication"

JAMES F. LEWKOWICZ
Contract Manager

HENRY A. OSSING
Branch Chief

FOR THE COMMANDER

DONALD H. ECKHARDT
Division Director

This report has been reviewed by the ESD Public Affairs Office (PA) and is releasable to the National Technical Information Service (NTIS).

Qualified requestors may obtain additional copies from the Defense Technical Information Center. All others should apply to the National Technical Information Service.

If your address has changed, or if you wish to be removed from the mailing list, or if the addressee is no longer employed by your organization, please notify AFGL/DAA, Hanscom AFB, MA 01731. This will assist us in maintaining a current mailing list.

Do not return copies of this report unless contractual obligations or notices on a specific document requires that it be returned.

UNCLASSIFIED
SECURITY CLASSIFICATION OF THIS PAGE

REPORT DOCUMENTATION PAGE AD-A181 455

Form Approved
OMB No 0704-0188
Exp Date Jun 30, 1986

1a REPORT SECURITY CLASSIFICATION Unclassified	1b RESTRICTIVE MARKINGS
2a SECURITY CLASSIFICATION AUTHORITY	3 DISTRIBUTION/AVAILABILITY OF REPORT approved for public release; distribution unlimited
2b DECLASSIFICATION/DOWNGRADING SCHEDULE	
4 PERFORMING ORGANIZATION REPORT NUMBER(S) TGAL-87-01	5 MONITORING ORGANIZATION REPORT NUMBER(S) AFGL-TR-87- 0106
6a NAME OF PERFORMING ORGANIZATION Teledyne Geotech 6b OFFICE SYMBOL (If applicable) TGAL	7a NAME OF MONITORING ORGANIZATION Air Force Geophysics Laboratory
6c ADDRESS (City, State, and ZIP Code) 314 Montgomery Street Alexandria, VA 22314-1581	7b ADDRESS (City, State, and ZIP Code) Hanscom AFB MA 01731-0035
8a NAME OF FUNDING/SPONSORING ORGANIZATION Air Force Geophysics Laboratory 8b OFFICE SYMBOL (If applicable) DSO/GSD	9 PROCUREMENT INSTRUMENT IDENTIFICATION NUMBER F19628-85C-0035
8c ADDRESS (City, State, and ZIP Code) Hanscom AFB MA 01731-5000	10 SOURCE OF FUNDING NUMBERS PROGRAM ELEMENT NO: 62714E PROJECT NO: 5A10 TASK NO: DA WORK UNIT ACCESSION NO: AX

11 TITLE (Include Security Classification)
Finite-Difference Modeling of Seismological Problems in Magnitude Estimation using Body Waves, Surface Waves, and Seismic Source Imaging

12 PERSONAL AUTHOR(S)
K. L. McLaughlin, Z. A. Der, R.-S. Jih, A. C. Lees, and L. M. Anderson

13a TYPE OF REPORT	13b TIME COVERED	14 DATE OF REPORT (Year, Month, Day)	15 PAGE COUNT
Final Report	FROM 2/11/85 to 2/10/87	March 1987	38

16 SUPPLEMENTARY NOTATION

17 COSATI CODES			18 SUBJECT TERMS (Continue on reverse if necessary and identify by block number)
FIELD	GROUP	SUB-GROUP	Finite-Difference, Synthetics, Scattering, Heterogeneity, Topography

19 ABSTRACT (Continue on reverse if necessary and identify by block number)

We briefly summarize in this final report the results from the three scientific reports delivered under this contract. Our work has focused on the effects of near-source heterogeneity upon seismic magnitude-yield determination. The basic tool in this work has been a developing 2-dimensional linear finite-difference code which computes the dynamic elastic response of an Earth model to specified initial conditions. By use of various initial conditions and the reciprocity theorem, we can generate the linear response of the Earth model to a general seismic source. Current work is limited to 2-D models and line sources. This FORTRAN-77 code has been run under the UNIX operating system on VAX, Cray, SUN, and Celerity. Major modifications on the code during this project include the addition of general free-surface boundary conditions capable of handling topography with slopes of any angle, as well as the fundamental mode Rayleigh wave packet adequate for numerical studies. Work on this program continues to increase it's performance, versatility, and portability.

20 DISTRIBUTION/AVAILABILITY OF ABSTRACT ☐ UNCLASSIFIED/UNLIMITED ☐ SAME AS RPT ☐ DTIC USERS	21 ABSTRACT SECURITY CLASSIFICATION Unclassified
22a NAME OF RESPONSIBLE INDIVIDUAL James F. Lewkowitz	22b TELEPHONE (Include Area Code) (617) 377-3028 22c OFFICE SYMBOL LWH

DD FORM 1473, 84 MAR — 83 APR edition may be used until exhausted. All other editions are obsolete

SECURITY CLASSIFICATION OF THIS PAGE
UNCLASSIFIED

(19. Continued)

Finite-difference simulations of P wave propagation through models of extreme topographic profiles of the southern Sahara test site were used to investigate the effect of topography on the variation of short-period m_b estimate of contained nuclear explosions. We have shown, as much as the 2-D assumption is valid, that the topography above the explosions RUBIS and SAPHIR could be responsible for suppressing the elastic pP. As part of the data analysis to support these calculations we have refined the attenuation estimate (spectral $\overline{t^*}$ estimate) for the southern Sahara test site and confirm that the attenuation bias between this test site and NTS should be minimal. Furthermore, we have used both spectral and deconvolution techniques to estimate far-field P-wave source time functions and explosion moments for SAPHIR, RUBIS, EMERAUDE, and GRENAT.

Synthetic teleseismic P-wave seismograms were also produced for a two dimensional, laterally heterogeneous model of Yucca Flats, NTS. This work shows that the geologic structure of Yucca Flats could be responsible for generation of the reverberant P coda and for teleseismic magnitude variations as large as 0.3 magnitude units. This structure would also make difficult the identification of elastic P+pP interference in the frequency domain. Indications are that m_b magnitude variations should be reduced by averaging over many azimuths and takeoff angles at teleseismic distance.

Finite-difference simulations were used to investigate the scattering of incident Rayleigh waves. Shallow explosions in layered media generate considerable more short-period Rayleigh wave energy than is observed, so the Rayleigh waves must be either attenuated by absorption or scattering. We find that reflection of Rayleigh waves by topographic features is an inefficient process and the bulk of the energy that is not transmitted as Rayleigh waves is converted to bodywaves. The scattering of these short-period Rayleigh waves into SV trapped in the crust as Lg or as P waves scattered into teleseismic P coda serve as possible models for the generation of Lg by explosions and the generation of teleseismic P coda near the source. Future work along this line is to compare the scattering from topography to that produced by shallow heterogeneity.

Recommendations for further work include:

(1) Extensions of the current finite difference code from 2-D to 3-D to study the attenuation of body waves by 3-D heterogeneity in the crust, test hypotheses about the generation of P coda and anisotropic P wave generation, and generation of transverse Lg by explosions.

(2) Introduction of other numerical methods to explore the coupling (scattering) of modes of wave-guide regional phases such as Pg and Lg, as well as the scattering of Pn and Sn. These methods include 2-D and 3-D scattering from localized heterogeneity as well as from rough boundaries.

(3) Coupling of efficient reflectivity methods to finite difference calculations to propagate the scattered field to regional distances and to drive the finite difference responses with realistic in-coming regional phases.

(4) Investigation of scattering of fundamental and higher mode short-period Rayleigh waves by 2-D topography and shallow heterogeneity with more realistic velocity gradients near the surface.

(5) Extension of the general topographic boundary condition to include the general fluid-solid interface for the modeling of scattering at rough fluid-solid boundaries.

SUMMARY

We briefly summarize in this final report the results from the three scientific reports delivered under this contract. Our work has focused on the effects of near-source heterogeneity upon seismic magnitude-yield determination. The basic tool in this work has been a developing 2-dimensional linear finite-difference code which computes the dynamic elastic response of an Earth model to specified initial conditions. By use of various initial conditions and the reciprocity theorem, we can generate the linear response of the Earth model to a general seismic source. Current work is limited to 2-D models and line sources. This FORTRAN-77 code has been run under the UNIX operating system on VAX, Cray, SUN, and Celerity. Major modifications on the code during this project include the addition of general free-surface boundary conditions capable of handling topography with slopes of any angle, as well as the fundamental mode Rayleigh wave packet adequate for numerical studies. Work on this program continues to increase it's performance, versatility, and portability.

Finite-difference simulations of P wave propagation through models of extreme topographic profiles of the southern Sahara test site were used to investigate the effect of topography on the variation of short-period m_b estimate of contained nuclear explosions. We have shown, as much as the 2-D assumption is valid, that the topography above the explosions RUBIS and SAPHIR could be responsible for suppressing the elastic pP. As part of the data analysis to support these calculations we have refined the attenuation estimate (spectral $\overline{t^*}$ estimate) for the southern Sahara test site and confirm that the attenuation bias between this test site and NTS should be minimal. Furthermore, we have used both spectral and deconvolution techniques to estimate far-field P-wave source time functions and explosion moments for SAPHIR, RUBIS, EMERAUDE, and GRENAT.

Synthetic teleseismic P-wave seismograms were also produced for a two dimensional, laterally heterogeneous model of Yucca Flats, NTS. This work shows that the geologic structure of Yucca Flats could be responsible for generation of the reverberant P coda and for teleseismic magnitude variations as large as 0.3 magnitude units. This structure would also make difficult the identification of elastic P+pP interference in the frequency domain. Indications are that m_b magnitude variations should be reduced by averaging over many azimuths and takeoff angles at teleseismic distance.

Finite-difference simulations were used to investigate the scattering of incident Rayleigh waves. Shallow explosions in layered media generate considerable more short-period Rayleigh wave energy than is observed, so the Rayleigh waves must be either attenuated by absorption or scattering. We find that reflection of Rayleigh waves by topographic features is an inefficient process and the bulk of the energy that is not transmitted as Rayleigh waves is converted to bodywaves. The scattering of these short-period Rayleigh waves into SV trapped in the crust as Lg or as P waves scattered into teleseismic P coda serve as possible models for the generation of Lg by explosions and the generation of teleseismic P coda near the source. Future work along this line is to compare the scattering from topography to that produced by shallow heterogeneity.

Recommendations for further work include:

(1) Extensions of the current finite difference code from 2-D to 3-D to study the attenuation of body waves by 3-D heterogeneity in the crust, test hypotheses about the generation of P coda and anisotropic P wave generation, and generation of transverse Lg by explosions.

(2) Introduction of other numerical methods to explore the coupling (scattering) of modes of wave-guide regional phases such as Pg and Lg, as well as the scattering of Pn and Sn. These methods include 2-D and 3-D scattering from localized heterogeneity as well as

from rough boundaries.

(3) Coupling of efficient reflectivity methods to finite difference calculations to propagate the scattered field to regional distances and to drive the finite difference responses with realistic in-coming regional phases.

(4) Investigation of scattering of fundamental and higher mode short-period Rayleigh waves by 2-D topography and shallow heterogeneity with more realistic velocity gradients near the surface.

(5) Extension of the general topographic boundary condition to include the general fluid-solid interface for the modeling of scattering at rough fluid-solid boundaries.

TABLE OF CONTENTS

BOUNDARY CONDITIONS FOR ARBITRARY POLYGONAL TOPOGRAPHY IN A 2-D ELASTIC FINITE-DIFFERENCE SCHEME FOR SEISMOGRAM GENERATION

Rong-Song Jih, Keith L. McLaughlin, and Zoltan A. Der
Teledyne Geotech Alexandria Laboratories
314 Montgomery Street
Alexandria, Virginia 22314-1581

ABSTRACT

A simple method to implement the free-surface topography of polygonal shape in 2-D explicit finite-difference simulations of the elastic wave equation is presented that includes an empirically stable treatment of various slopes and transition points between the sloping segments.

On the inclined free surface, the vanishing stress conditions are implemented to a rotated coordinate system parallel to the inclined boundary as previous works did. While for each transition point on the topography where the slope changes, we propose to use the first-order approximation of boundary conditions in a locally rotated coordinate system in which the normal axis always coincides with the bisector of the corner. This mixed algorithm is stable for Poisson ratios of practical interest and thus enables us to study a wide range of problems where the topography plays a significant role in shaping the wavefield. Examples are shown simulating the propagation of P and Rayleigh waves traveling through a model with a 45^o ramp and a mountain shape as the free surface. By using reciprocity principle and appropriate deconvolutions on the seismograms generated in this scheme, the effect of complicated near-source topography on the far-field teleseismic waveforms can be characterized.

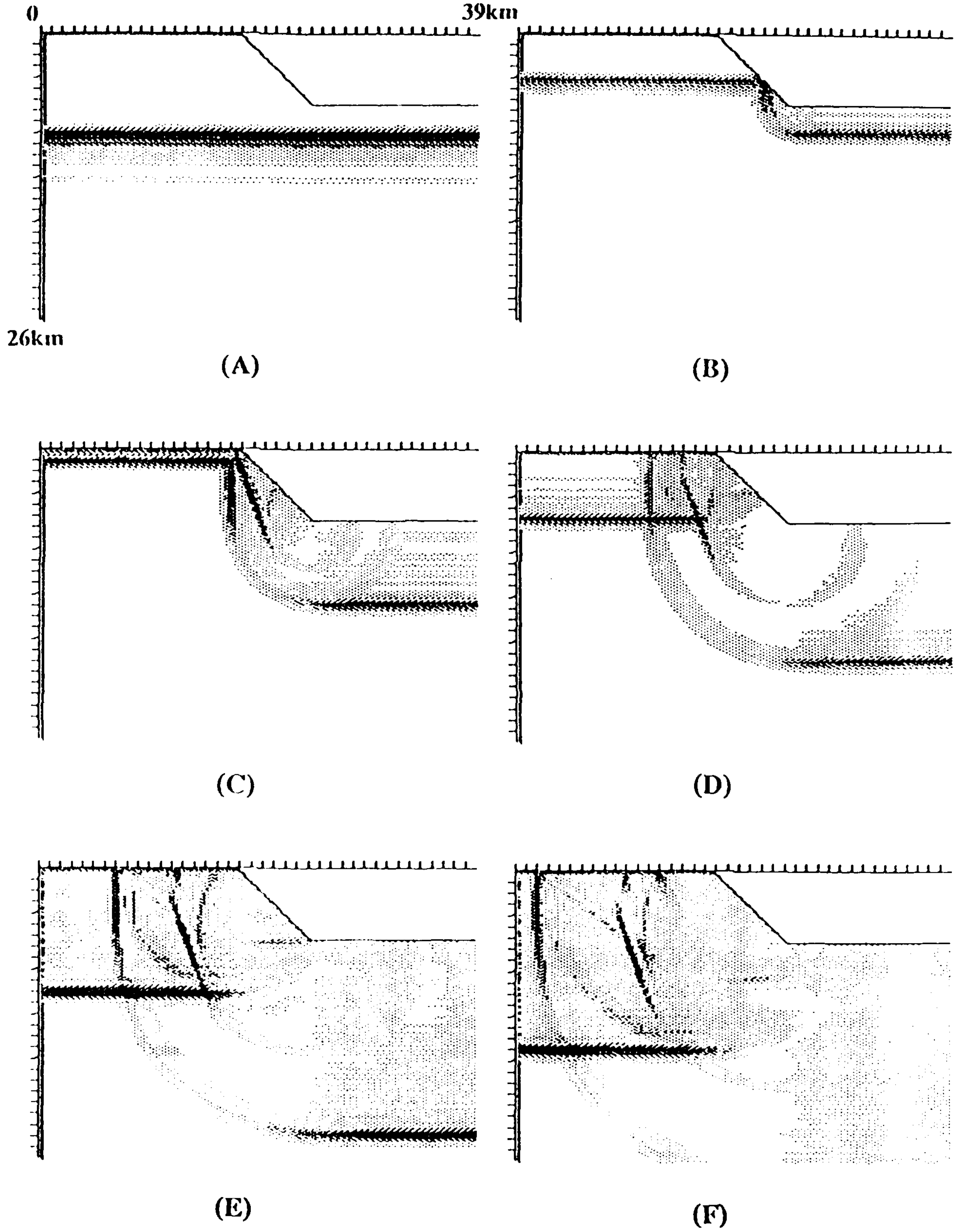

Figure 1.1 The propagation of a normally incident broadband plane P wave through a model with a 45° ramp on the top of grid and symmetric boundary condition used on both sides. Shading is proportional to displacement amplitude. The appropriate P-S conversions and reflections, diffractions satisfying Snell's law and Huygen's principle are clearly visible in these successive snapshots taken every second.

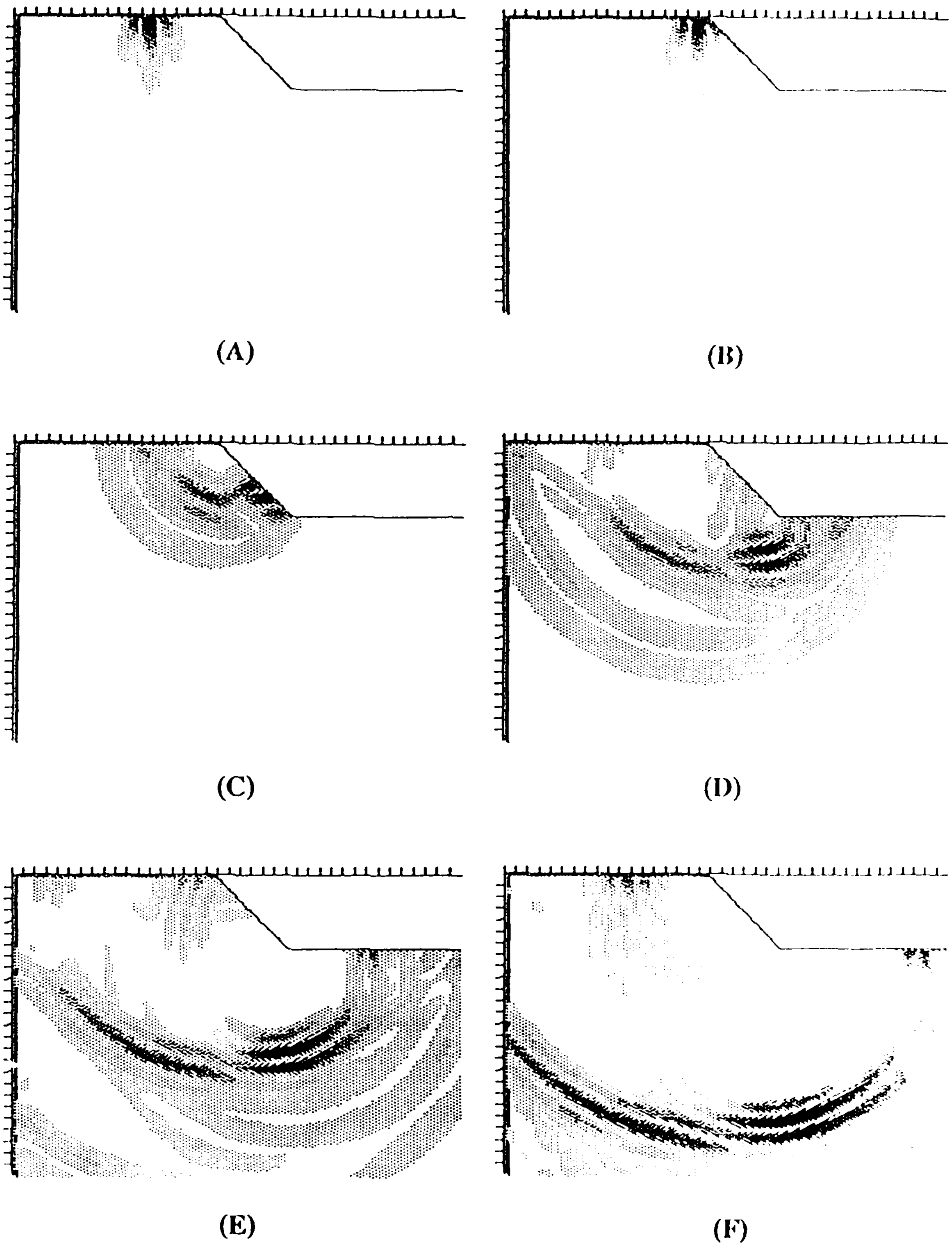

Figure 1.2 Same topographic configuration as in Figure 1.1 with Ricker wavelet-shaped Rayleigh wave of fundamental mode propagating from left side of the grid. When the incident wave packet encounters the corner points of the ramp, the diffraction patterns look like radiation due to point source at corners. Most energy of the incident Rayleigh wave is scattered as body waves and absorbed by the quasi-transparent boundary conditions used in this simulation.

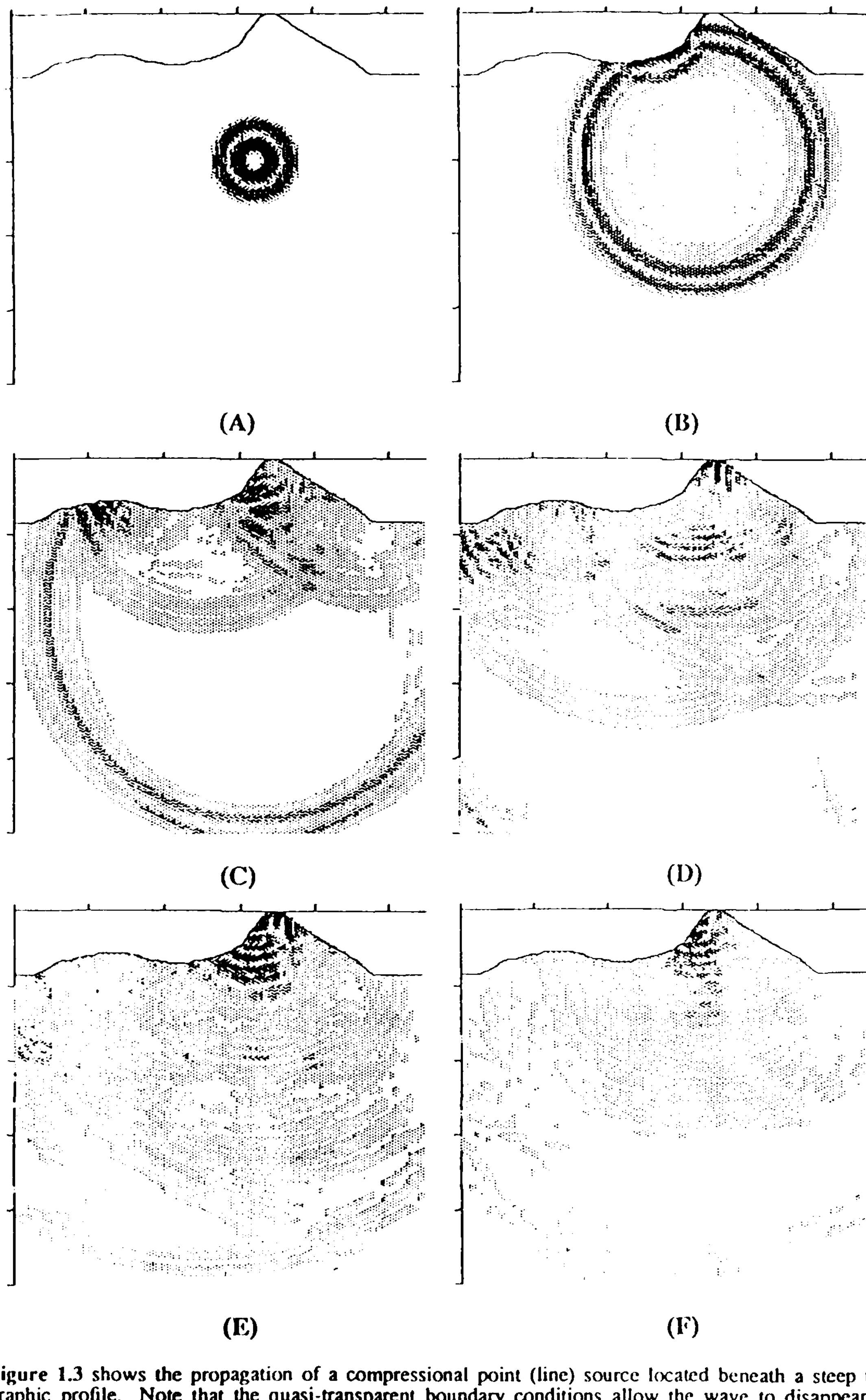

Figure 1.3 shows the propagation of a compressional point (line) source located beneath a steep topographic profile. Note that the quasi-transparent boundary conditions allow the wave to disappear into the sides and bottom of the grid. Snapshots are separated by 0.25 second.

TELESEISMIC SPECTRAL AND TEMPORAL M_o AND Ψ_∞ ESTIMATES FOR FOUR FRENCH EXPLOSIONS IN SOUTHERN SAHARA

Keith L. McLaughlin, Alison C. Lees, and Zoltan A. Der
Teledyne Geotech Alexandria Laboratories
314 Montgomery Street
Alexandria, Virginia 22314-1581

ABSTRACT

Estimates for explosion moment, M_o, and reduced displacement potential, Ψ_∞, are made for four French explosions at Taourirt Tan Afella Massif in southern French Sahara using data from the LRSM network and the arrays EKA and YKA. Preparatory to determining moments, $\overline{t^*}$ estimates are made for each station and the source region $\overline{t^*}$ values of 0.30 to 0.35 seconds are found for the southern Sahara test site. This source region attenuation level is consistent with the "hot spot" hypothesis for the Ahaggar plateau in northern Africa. Consequently, the attenuation bias between Ahaggar and the Nevada Test Site should be small.

Both spectral estimation and broadband temporal deconvolution methods are used for estimation of the explosion moments. The deconvolution estimates of static moment are found to be consistent with the spectral estimation methods. Deconvolved seismograms for the explosions EMERAUDE, RUBIS, SAPHIR, and GRENAT show evidence of strong anisotropic free surface interaction that may be due to scattering from the steep topography of the Taourirt Tan Affela Massif test site.

LRSM SPECTRAL MOMENT ESTIMATES 10^{24} dyne-cm				
EVENT	MEAN	RMS	GEOMETRIC MEAN	MEDIAN
RUBIS	0.064(0.01)	0.072	0.056	0.059
SAPHIR	0.30(0.10)	0.42	0.19	0.16

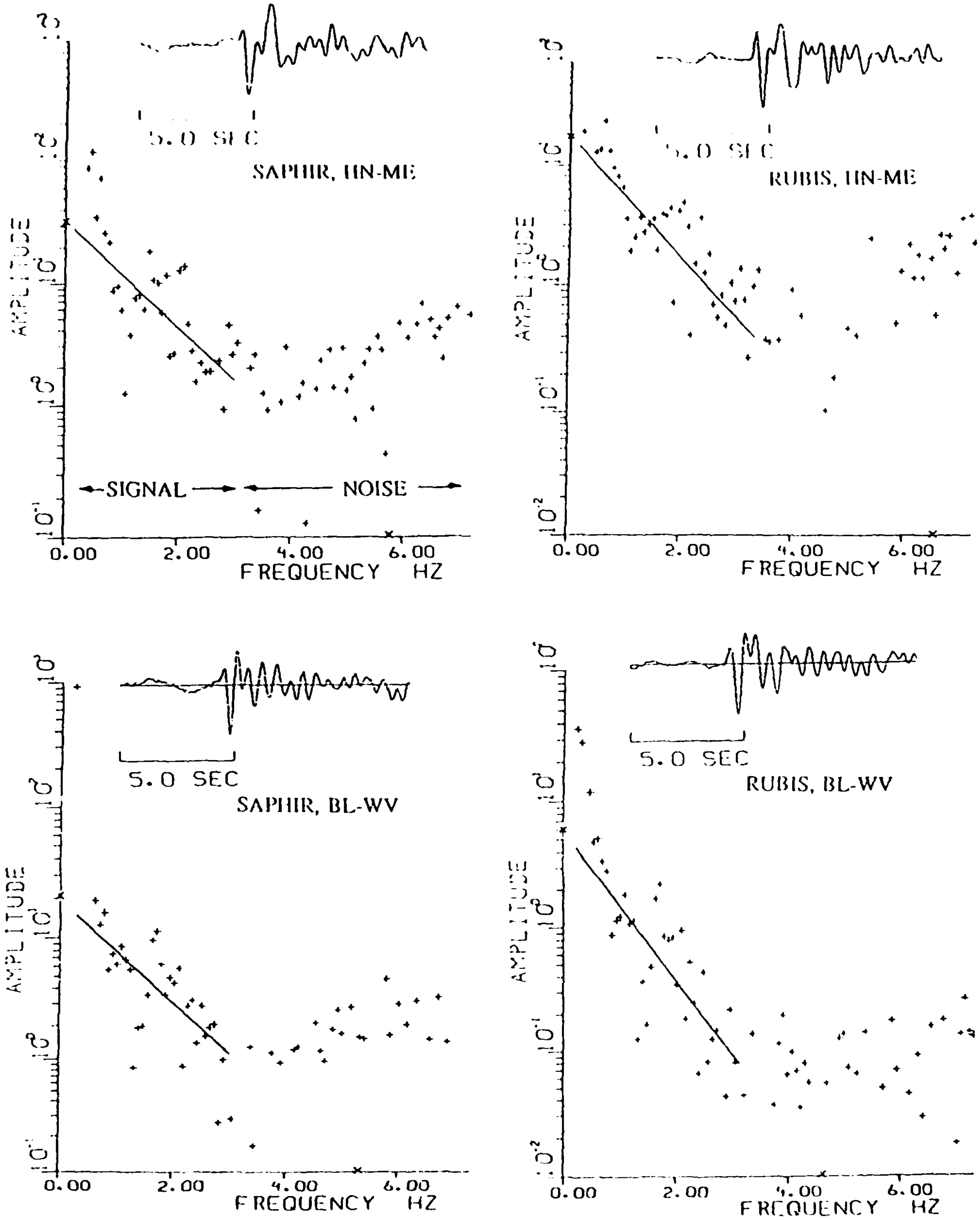

Figure 2.1 Spectra corrected for instrument and RDP. Slopes between 0.5 and 3.0 Hz are estimates of t^*, intercepts are estimates of Ω_o. Only spectral levels with an estimated signal-to-noise power ratio greater than 2 were used.

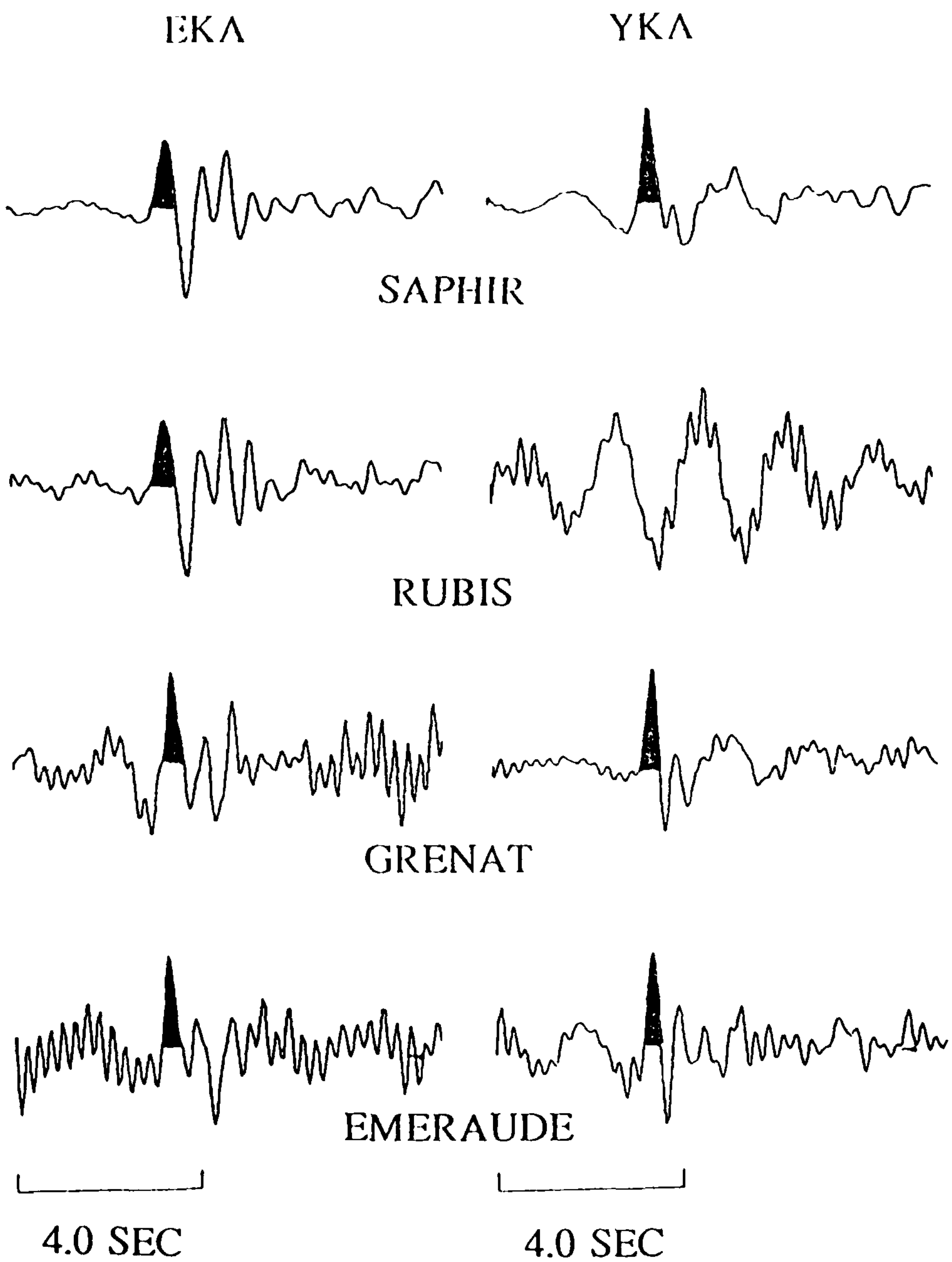

Figure 2.2 Deconvolved source time functions at the EKA and YKA arrays for SAPHIR, RUBIS, GRENAT and EMERAUDE. RUBIS was poorly recorded across YKA.

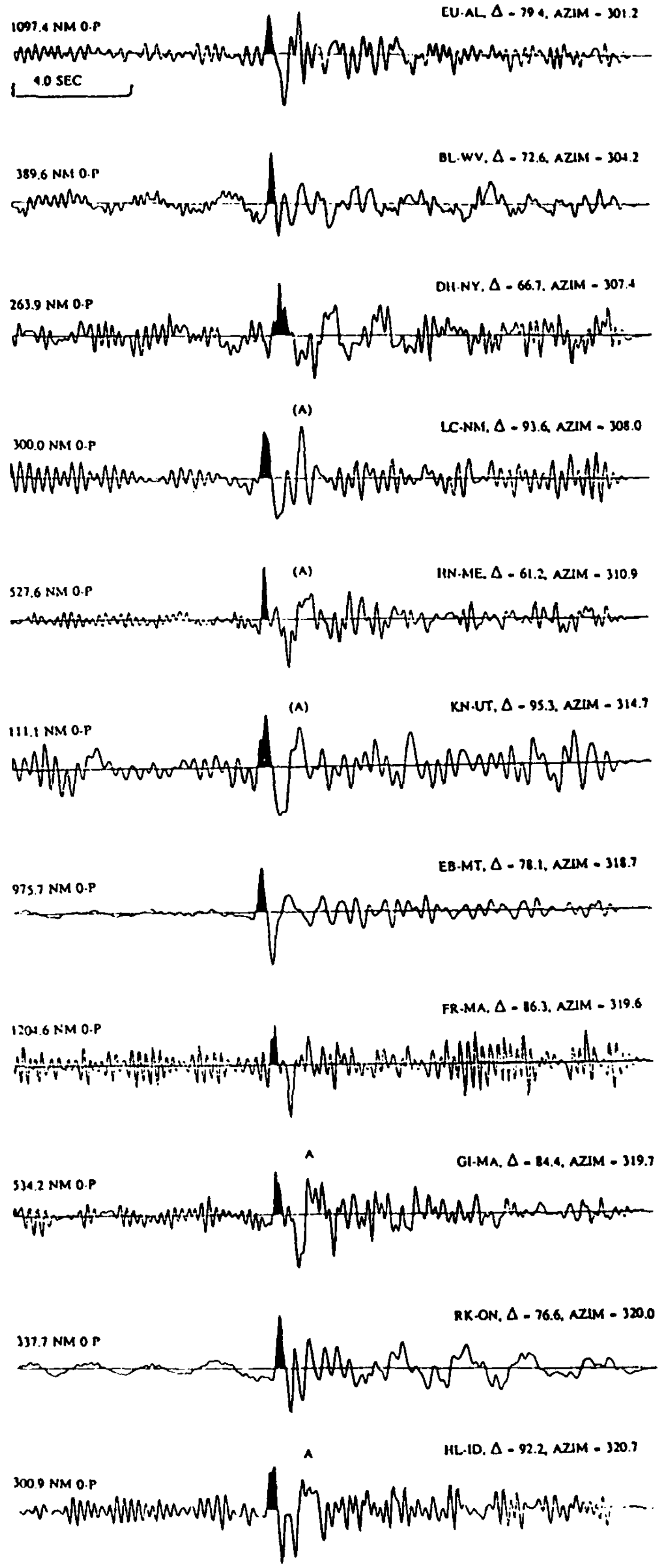

Figure 2.3 Deconvolved waveforms for RUBIS at LRSM stations. The causal P-wave pulse area is indicated for each trace. Traces are ordered in decreasing azimuth from the top. Late positive arrivals that may be correlated between stations are indicated by labels "A" and "(A)".

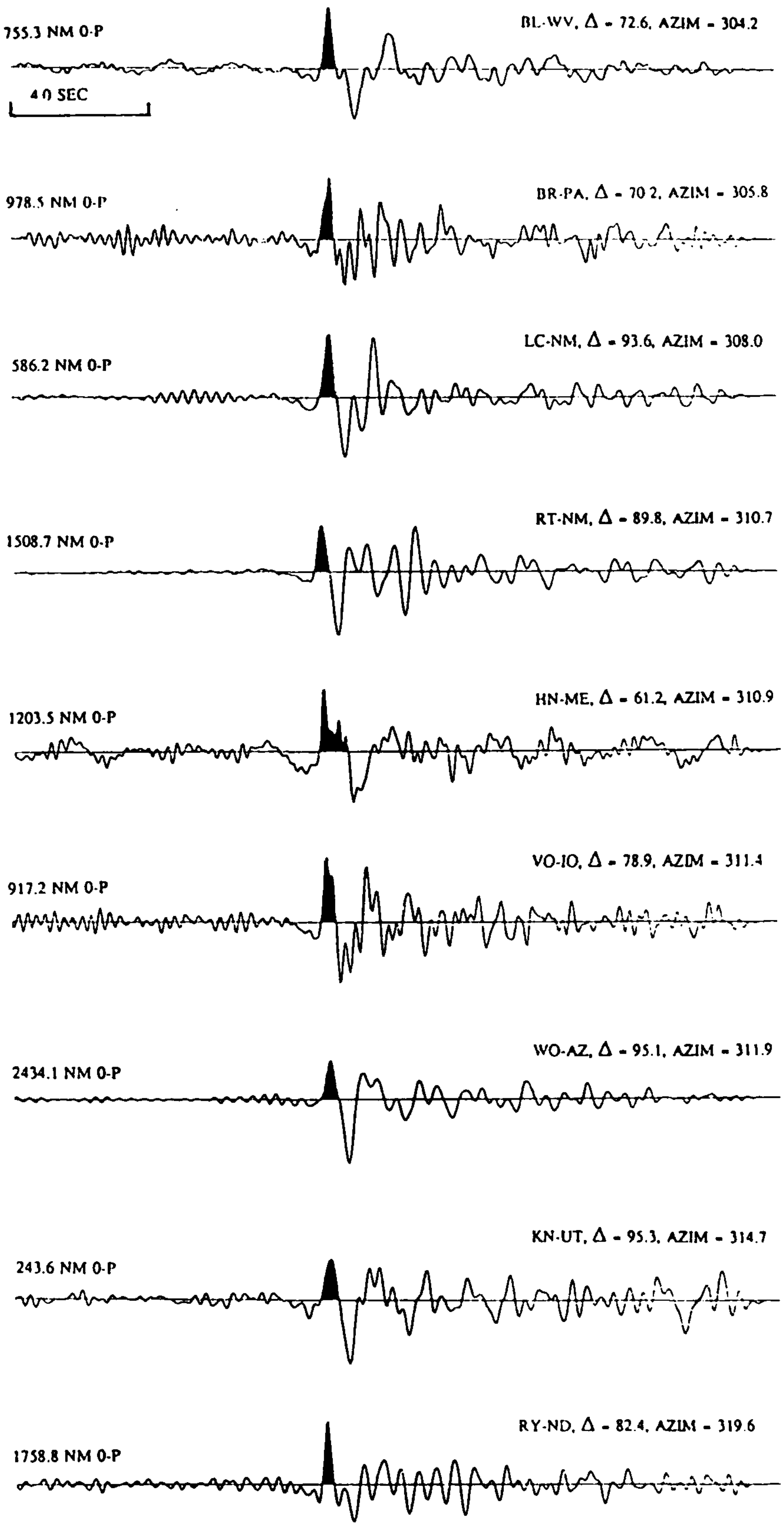

Figure 2.4 Deconvolved waveforms for SAPHIR at LRSM stations. The causal P-wave pulse area is indicated for each trace. Traces are ordered in decreasing azimuth from the top. The HN-ME waveform shows considerable broadening that may be due to a positive secondary arrival unique to the HN-ME station.

SCATTERING FROM NEAR-SOURCE TOPOGRAPHY: TELESEISMIC OBSERVATIONS AND NUMERICAL 2-D EXPLOSIVE LINE SOURCE SIMULATIONS

Keith Lynn McLaughlin and Rong-Song Jih
Teledyne Geotech Alexandria Labs
314 Montgomery Street
Alexandria, Virginia 22314-1581

ABSTRACT

2-D linear elastic finite-difference simulations of teleseismic P waveforms from line sources have been used to explore the variations that may be induced in event magnitude-yield determination by the emplacement of explosive sources under mountainous topographic features. The southern Sahara French test site in Algeria, at Taourirt Tan Afella Massif on the Ahaggar plateau has been used as a case study. The topography of this test site is extreme and the event locations permit a test of the hypothesis that topography influences short-period event magnitudes of contained nuclear explosions. The maximum variation that is expected is plus or minus 0.15 magnitude units from the network mean. The magnitude variations are expected to change rapidly with takeoff angle and azimuth.

Teleseismic observations of the explosions at the southern Sahara test site are compared to predictions made from 2-D simulations. Waveform data from the arrays EKA, and YKA as well as LRSM data have been deconvolved to broadband displacement for inspection of the apparent far-field P-wave source. Qualitative comparisons are favorable that the topography above the explosions RUBIS and SAPHIR defocused teleseismic pP at certain takeoff angles and azimuths. Long-period positive-polarity pulses can be seen at several sites that may indicate Rayleigh-to-P scattering from topography near the source.

WWSSN maximum likelihood magnitude data for the "a", "ab", and "max" P phases have been used to estimate that the magnitude variation due to topographic scattering is no more than 0.15 rms magnitude units across the WWSSN.

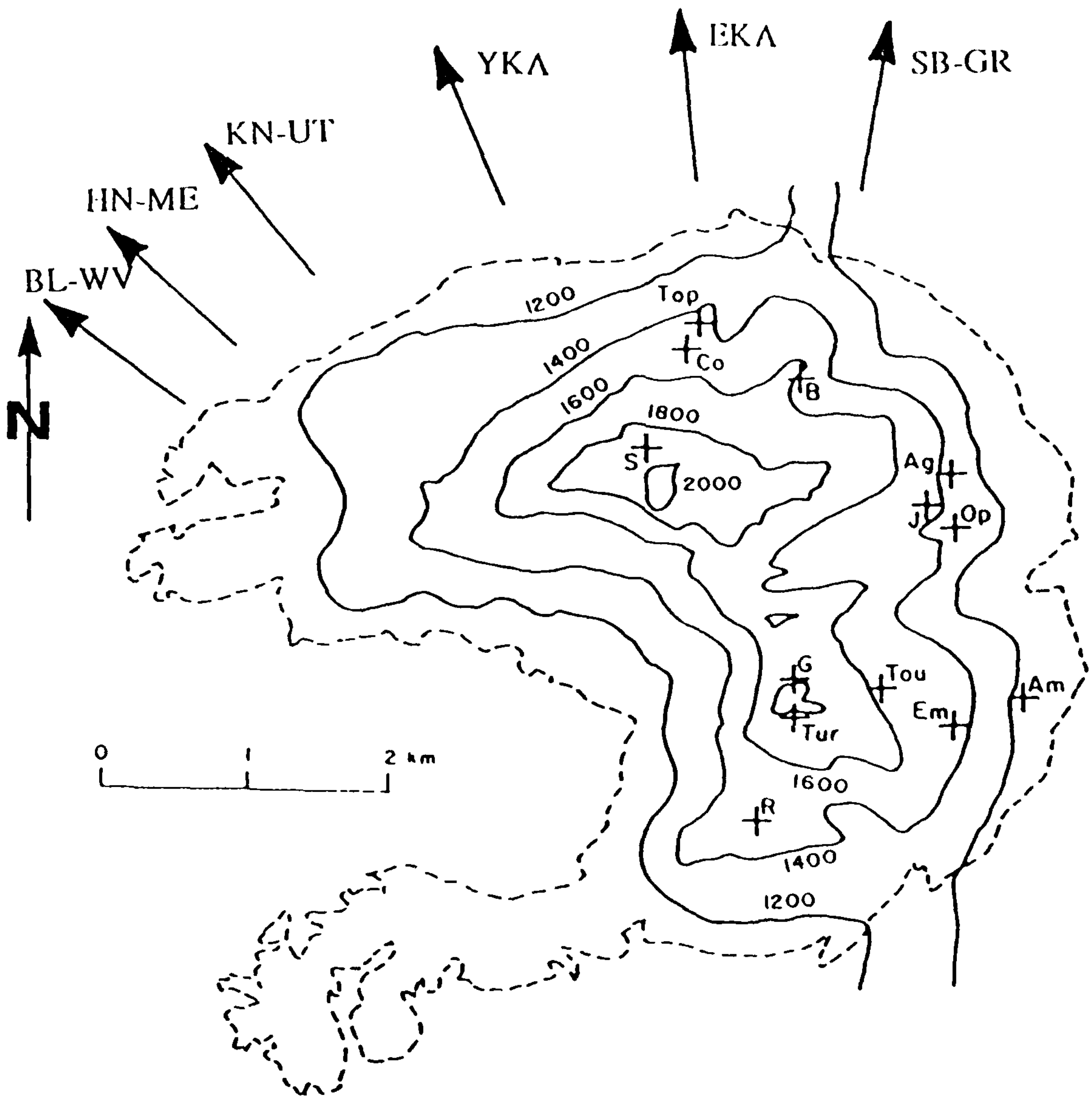

Figure 3.1 Topographic map Taourirt Tan Afella Massif from Duclaux and Michaud (1970) with event locations from Faure (1972) for SAPHIR (S), RUBIS (R), EMERAUDE (E), and GRENAT (G). Contours are 100 meters. The dashed line is the outcrop of the Taourirt Tan Afella Massif granite. Azimuths to several stations and arrays are indicated.

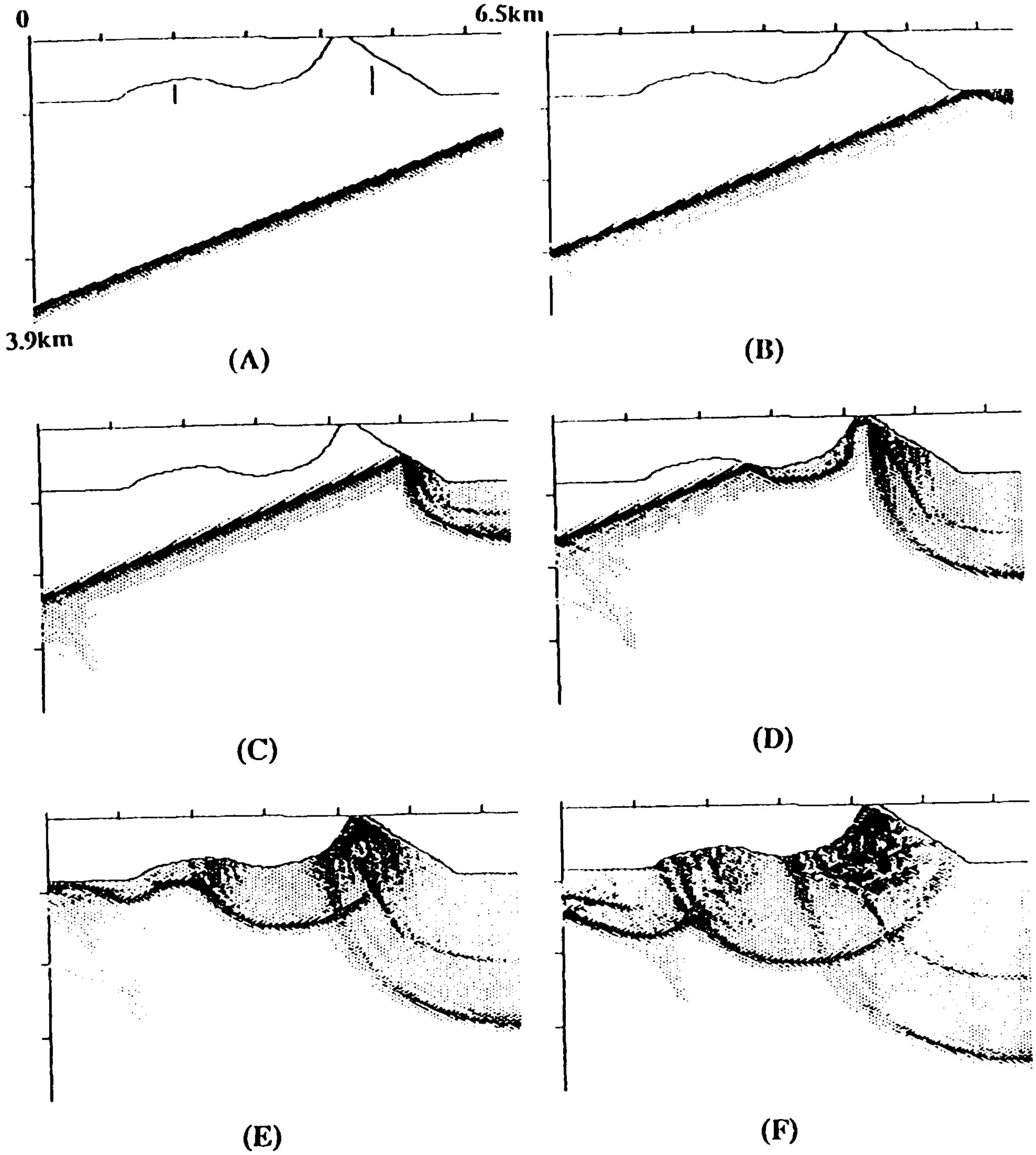

Figure 3.2 The displacement fields generated by a broadband plane P wave (*i.e.* source at infinity) of incidence angle 20° in a grid with steep topographic configuration. The topography is a (due north 344°) cross section of Taourirt Tan Afella Massif in southern Algeria. The successive frames separated by 0.125 sec show the initialization of the wave (A), P-reflection followed by S wave starting at right (B,C), completely developed reflections from all parts of the topography (E) and complex wavefields containing reflections, diffractions and possibly excited surface waves (E,F). It can be observed that the free-surface reflection is severely altered due to scattering from the free-surface. Far-field seismograms with compressional sources at locations beneath this topographic profile (black spots in (A)) can be derived by reciprocity.

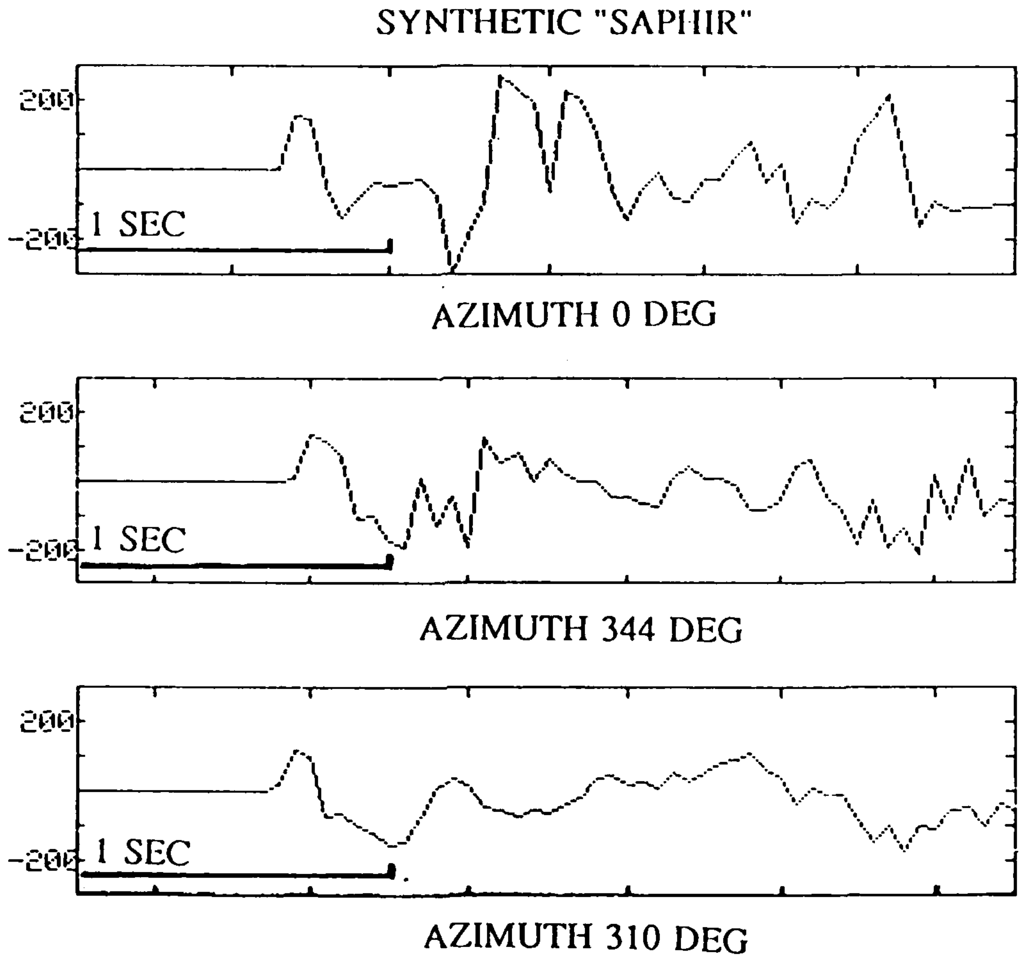

Figure 3.3 Synthetic teleseismic P waves (takeoff angle of 20 degrees) for the 2-D "SAPHIR" models at azimuths of 310, 344, and 0 degrees. Synthetics have only been convolved with an explosion source time function. No distinct well defined elastic pP is apparent although, several long-period complicated negative pulses can be seen to follow the initial P wave. Large positive secondary arrivals can be seen 0.5 sec following the initial P wave at 0 degrees azimuth.

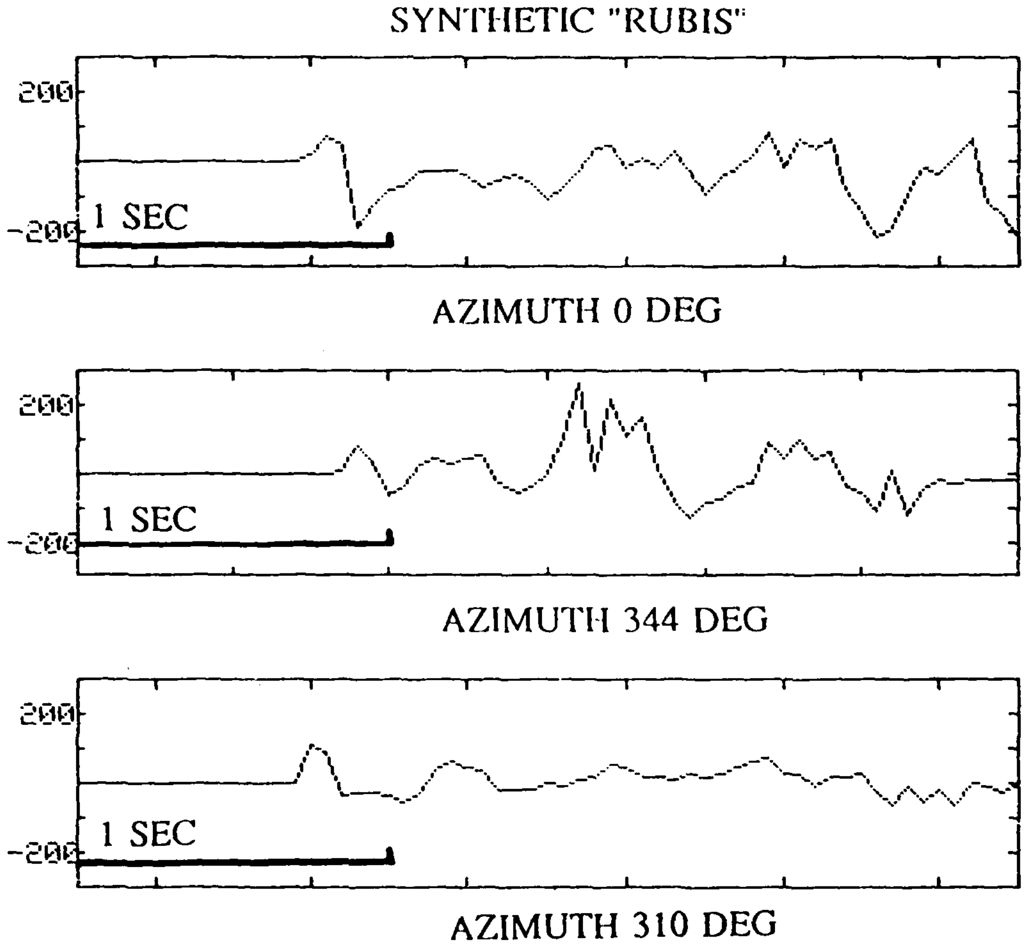

Figure 3.4 Synthetic teleseismic P waves (takeoff angle of 20 degrees) for the 2-D "RUBIS" models at azimuths of 310, 344, and 0 degrees. Synthetics have only been convolved with an explosion source time function. A distinct well defined elastic pP is only apparent for the azimuth of 0 degrees. Large positive pulses can be seen about 1 second after the P wave for the azimuth of 344 degrees.

EFFECTS OF LOCAL GEOLOGIC STRUCTURE ON YUCCA FLATS, NTS, EXPLOSION WAVEFORMS: 2-DIMENSIONAL LINEAR FINITE-DIFFERENCE SIMULATIONS

Keith L. McLaughlin, Lisa M. Anderson, and Alison C. Lees
Teledyne Geotech Alexandria Laboratories
314 Montgomery Street
Alexandria, Virginia 22314-1581

ABSTRACT

Two-dimensional linear elastic finite-difference calculations were performed for a two-dimensional geologic model of Yucca Flats, Nevada Test Site, Nevada. The calculations were used to produce synthetic teleseismic P-wave seismograms for explosive line sources in Yucca Flats. P-wave coda (first 5 seconds) is observed to be highly dependent on takeoff angle for the teleseismic synthetics. P-wave coda also varies with the position of the source in the valley structure and may produce variations in the individual station teleseismic P-wave m_b magnitude of up to 0.3 magnitude units. However these magnitude variations should be substantially reduced by averaging over stations at multiple azimuths.

The reverberant coda appears to arise from scattered modal waves that are initially excited in the low velocity near-surface structures of the Yucca Flats deposits of alluvium and tuff. Scattering of the waves occurs at offsets in the basement structure and the at the sides of the valley.

The combined effects of scattering, source function, intrinsic attenuation, and instrument response serve to obscure the P+pP spectral scalloping that is expected from a linear model. This loss of spectral resolution is the product of P coda filling in the P+pP interference notches and the lengthening of the initial P wave source time function by the convolution of the source time function, intrinsic attenuation operator and instrument response. Therefore, short time windows that do not include P coda energy do not have sufficient resolution to reliably detect the P+pP interference notches.

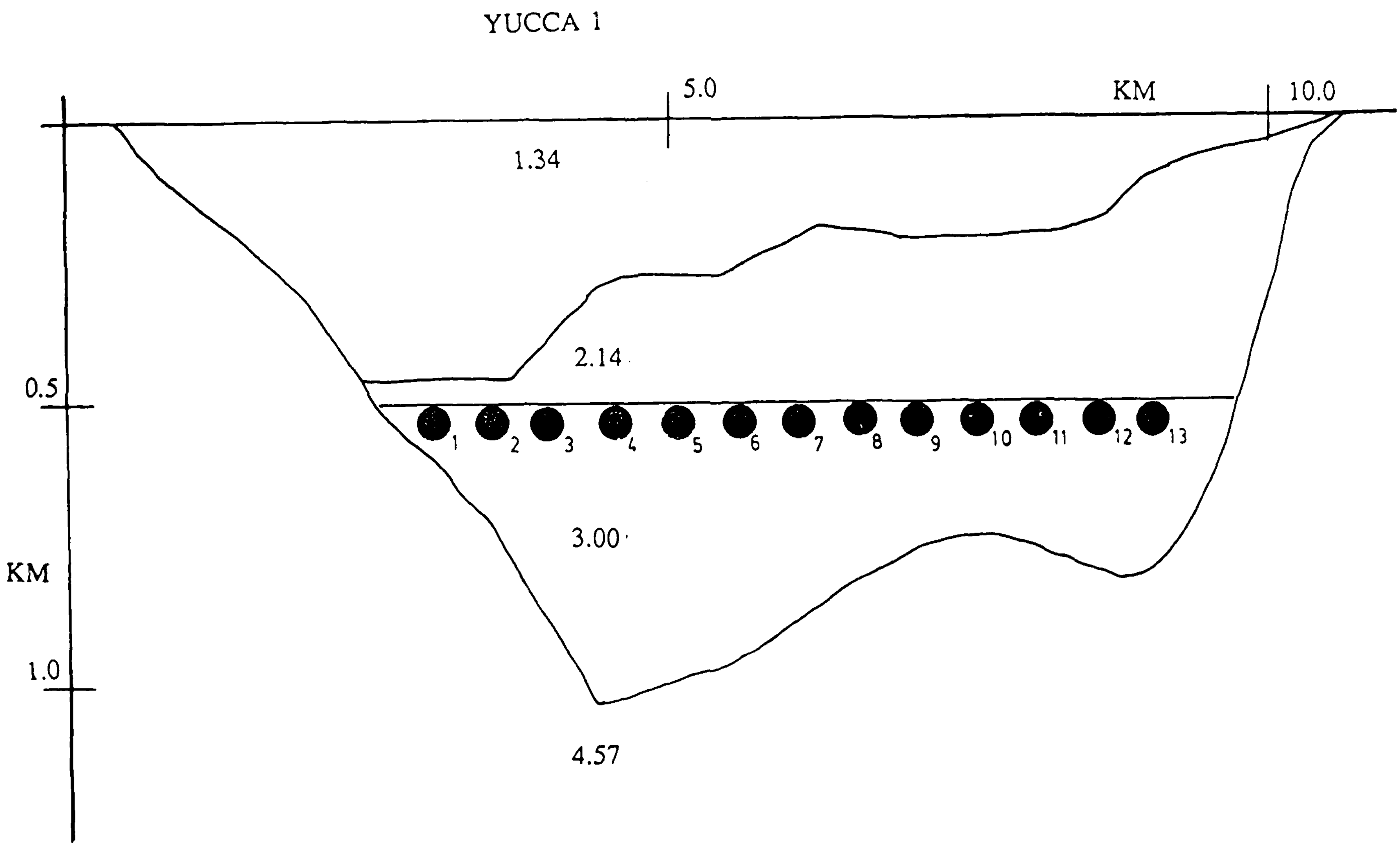

Figure 4.1 West-to-East model for geologic structure across Yucca Flats from Ferguson (1983). Model shown with 5-to-1 vertical exaggeration. Numbered source locations referred to in the text are indicated by solid dots at a depth of 550 meters below the surface. P-wave velocities of 1.34, 2.14, 3.00, and 4.57 km/sec are indicated for the geologic units of alluvium, unsaturated tuff, saturated tuff, and Paleozoic carbonates respectively.

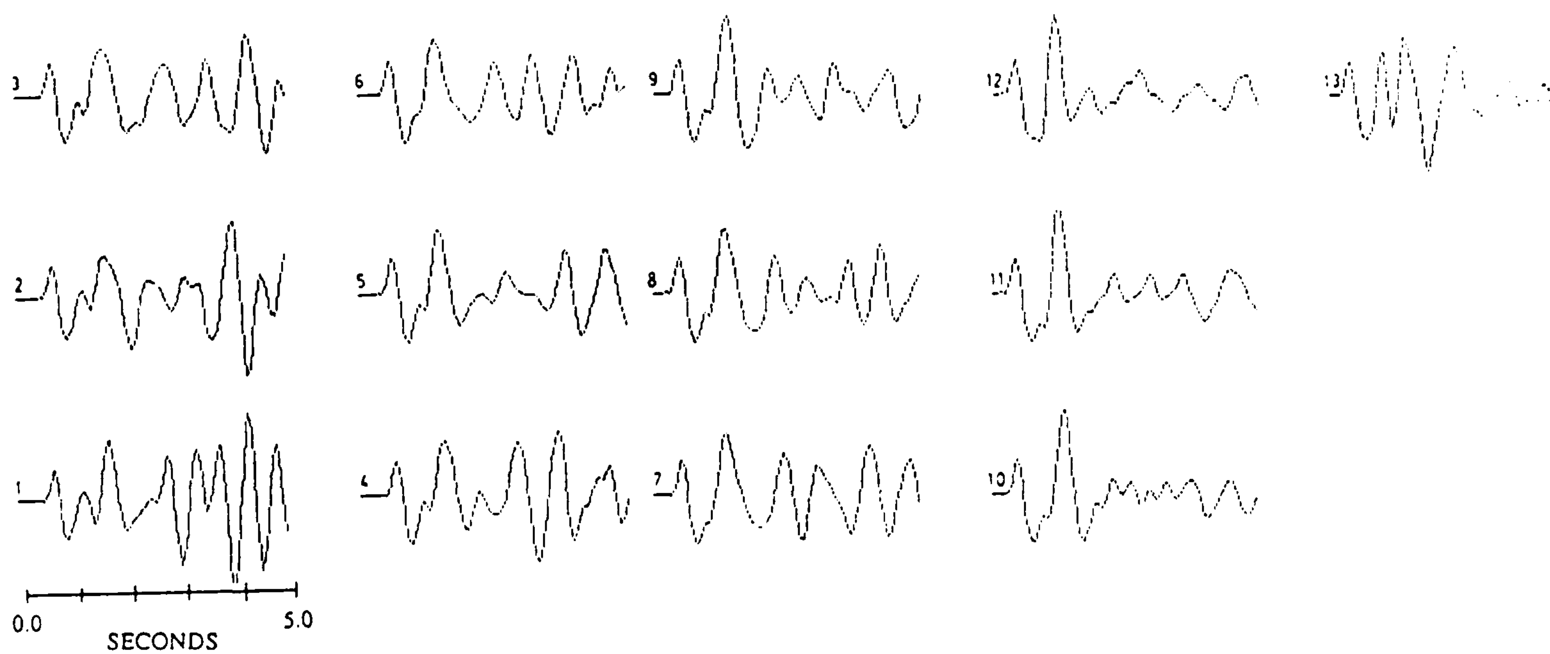

Figure 4.2 Teleseismic P-wave synthetics appropriate for a takeoff angle of 15 degrees for model in Figure 1. Numbers correspond to numbered source locations in Figure 1. 5 seconds of record are shown in each case. All synthetics are plotted at the same scale. Synthetics are calculated for a von Seggern Blandford (1972) hard rock 100 Kt RDP convolved with an instrument response and an attenuation operator as in FIGURE 2.

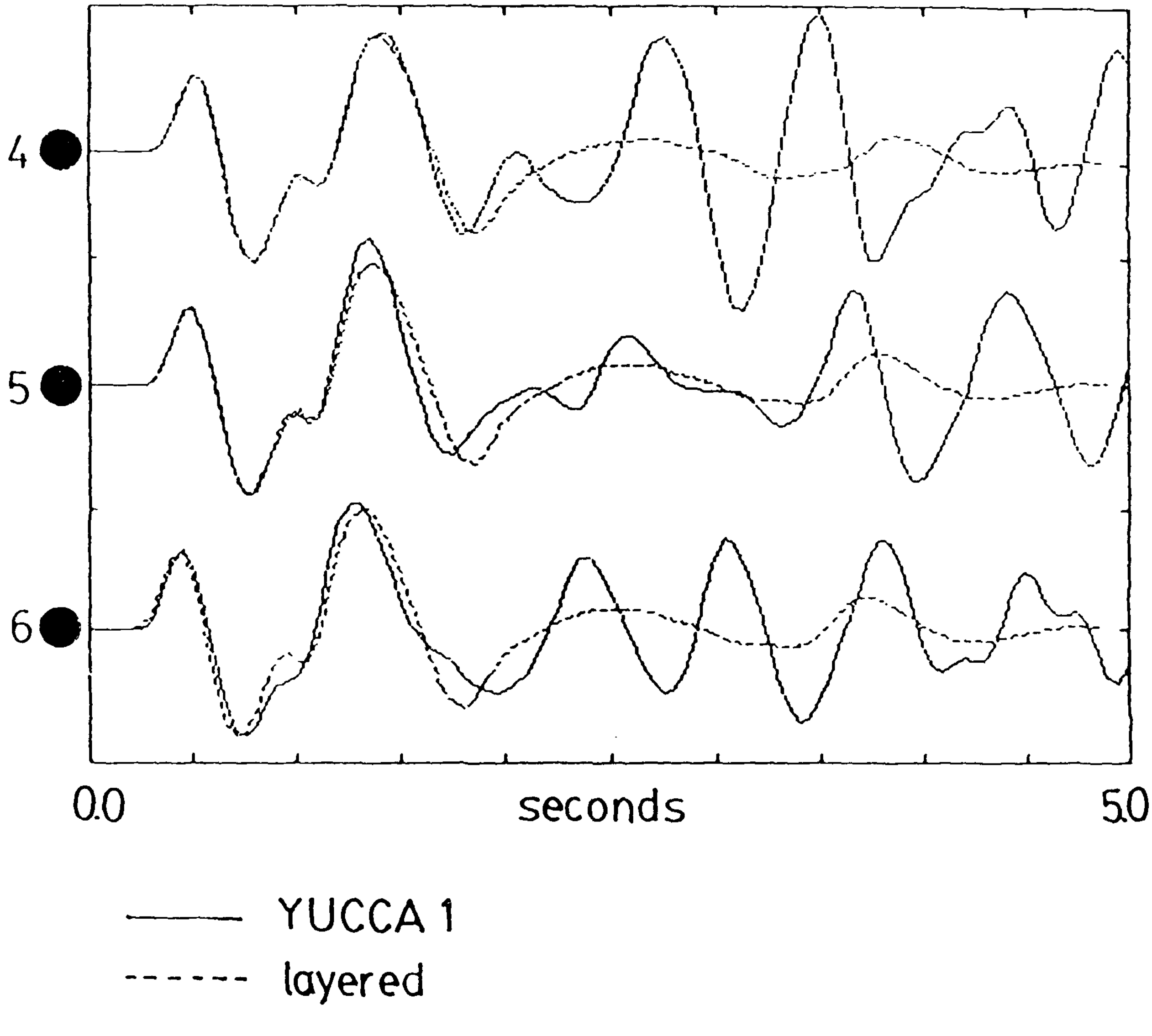

Figure 4.3 Synthetics for source locations 4, 5, and 6 at takeoff angle of 15 degrees compared to the layered model.

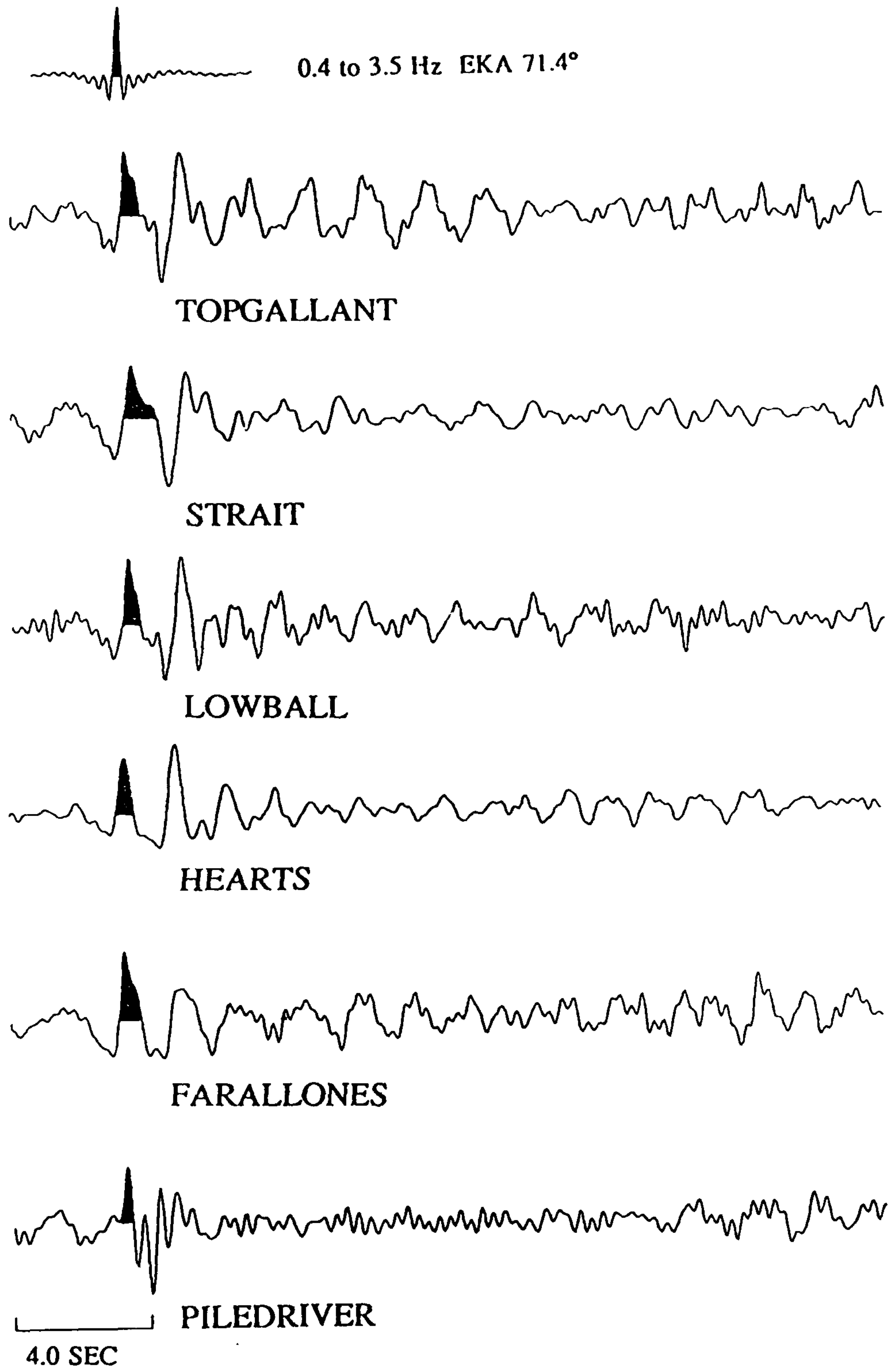

Figure 4.4 Deconvolved source time functions (far-field displacement) of Yucca Flats events and Piledriver at EKA array (Δ=71.4°). The effects of a constant t^*=0.45 sec attenuation operator have been removed. A resolution kernel is shown at the top representing the limited bandwidth of the deconvolutions, 0.4 to 3.5 Hz. The initial causal P wave has been been shaded for clarity. Note the higher frequency and shorter duration source time function of Piledriver with respect to the Yucca Flats events. Topgallant, Lowball, and Farallones have considerable reverberation in the first 5 seconds of record. The Yucca Flats events do not show a clear pP within 1 second of the initial P wave, although several events do show a negative phase about 1 second following the P wave and a positive pulse about 1.5 seconds following the P wave. Piledriver shows a negative pulse about 0.25 seconds following the P wave (pP?) and another negative polarity pulse about 0.8 seconds following the P wave.

FINITE-DIFFERENCE SIMULATIONS OF RAYLEIGH WAVE SCATTERING BY 2-D ROUGH TOPOGRAPHY

Keith Lynn McLaughlin and Rong-Song Jih
Teledyne Geotech Alexandria Labs
314 Montgomery Street
Alexandria, Virginia 22314-1581

ABSTRACT

Rayleigh waves normally incident upon 2-D simple or rough topographic structures are simulated by the linear finite-difference method to study the attenuation, transmission, and reflection of Rayleigh waves and to measure the Rayleigh-to-P and -SV bodywave conversion. For simple ramp structures, transmission, reflection, and scattering depend on the sign of change of slope of the topographic feature, as well as the ratio of the ramp height to the wavelength, h/λ. Simple ramp structures produce back-scattered bodywaves for $h>\lambda$, and forward-scattered bodywaves for $h<\lambda$. The radiation patterns of P and S bodywaves are roughly consistent with the model of equivalent point forces along the free surface. More complicated topographic features generated by random Markov sequences have been characterized by the Rayleigh-wave spatial Q(f). As expected, rougher topography attenuates Rayleigh waves more than smooth topography. P and S ampiitudes ratios are consistent with radiation from equivalent point forces near the surface, but the distribution of slownesses generated is greater than from the simple ramp structures. Reflection of Rayleigh waves by topographic slopes and by random topography is an inefficient process and the bulk of the energy that is not transmitted as Rayleigh waves is converted to bodywaves. Fundamental Rayleigh-to-Lg scattering and generation of teleseismic P coda by short period Rayleigh should be observable.

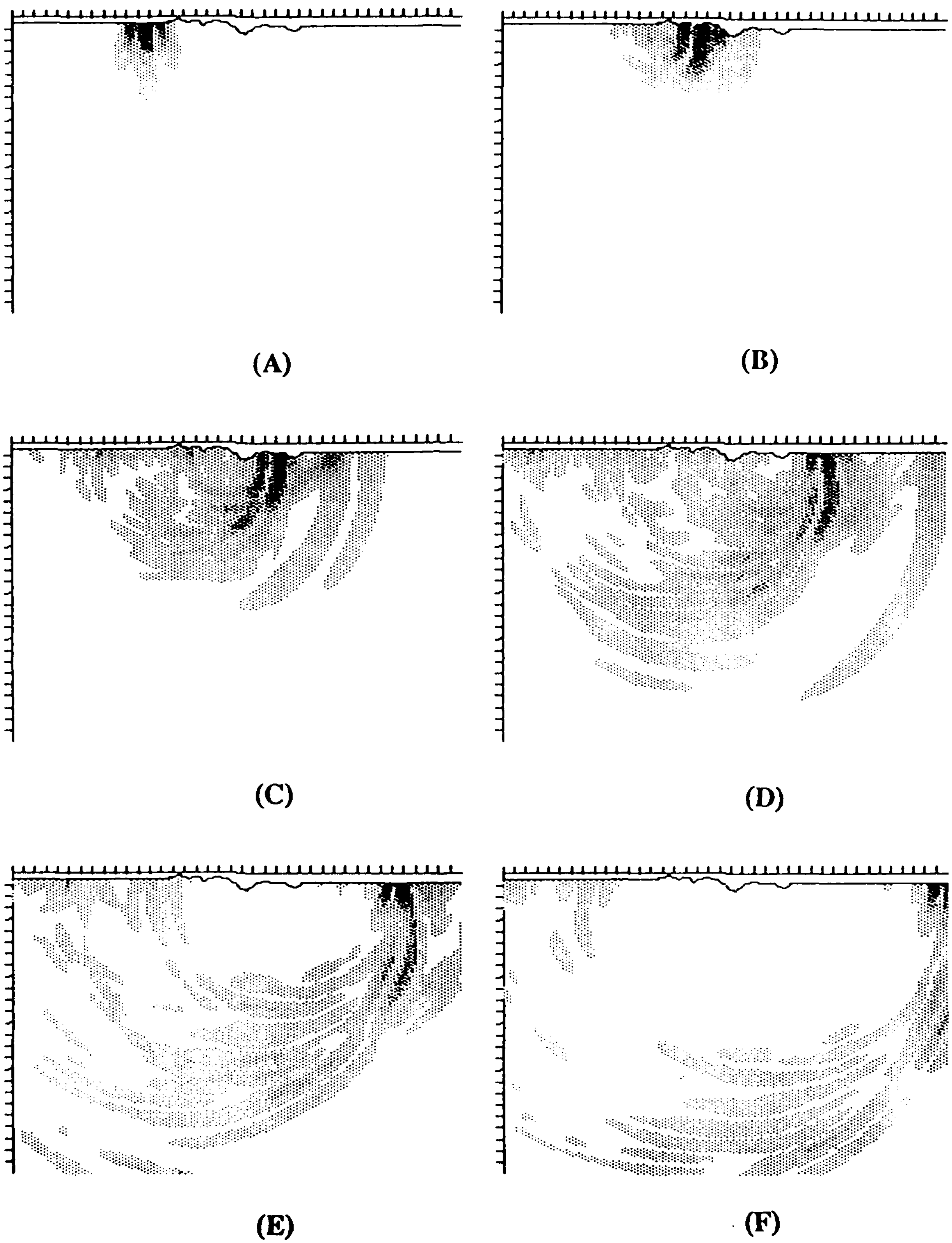

(A) (B) (C) (D) (E) (F)

Figure 5.1 Rayleigh wave incident on a rough topographic profile superimposed on a grid with absorbing boundary conditions for the sides and the bottom. Figures (A) through (F) correspond to displacement wavefields at distinct times with a temporal spacing of 2 sec. Note that the high frequency scattering of Rayleigh wave is *forward*.

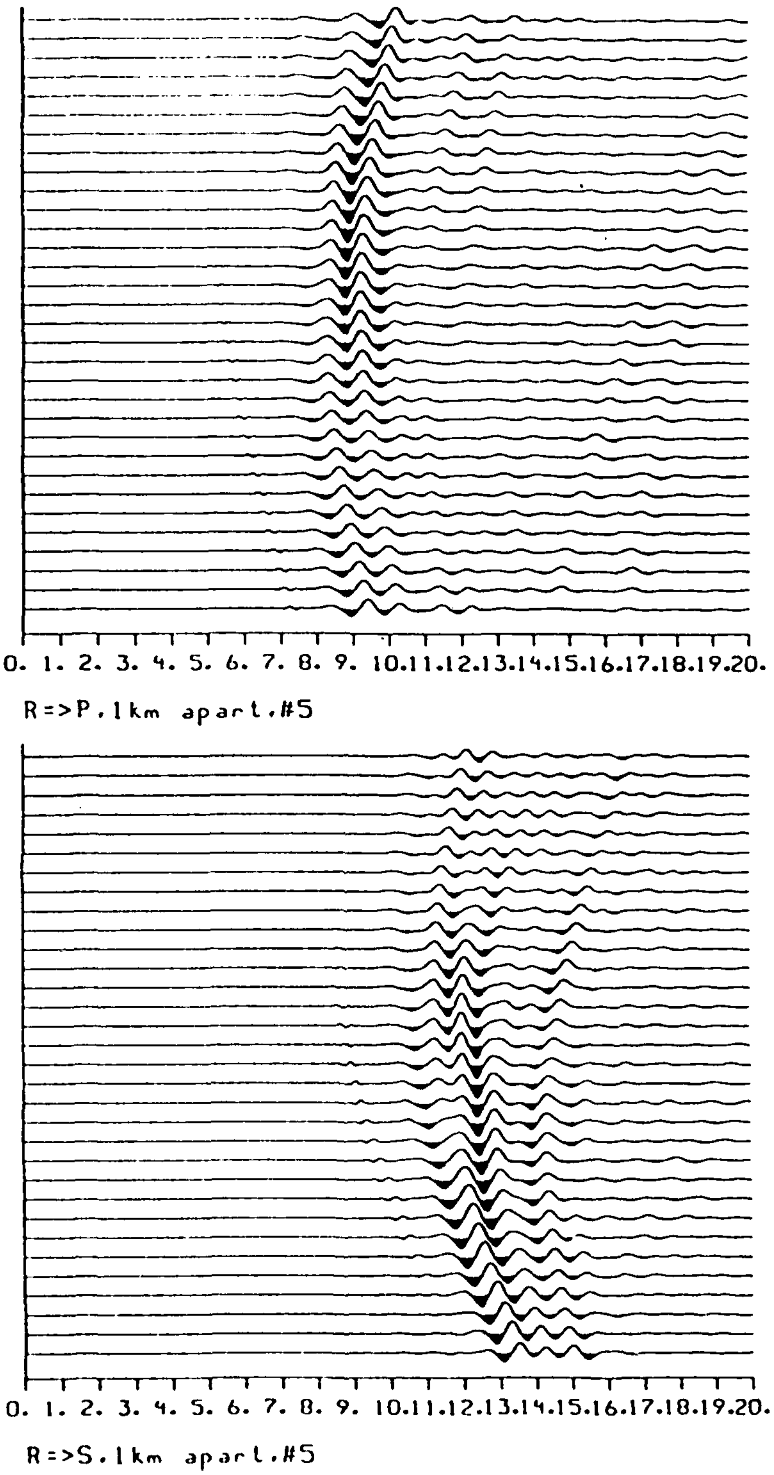

Figure 5.2 Seismic sections recording the converted P wave (dilatational strain, upper) and S wave (rotational strain, below) at a line of 32 sensors located near the bottom of the grid spaced 1 km apart for the same rough topography (#5)as in previous figure. Complicated interference patterns are evident for both P and S wavefields.

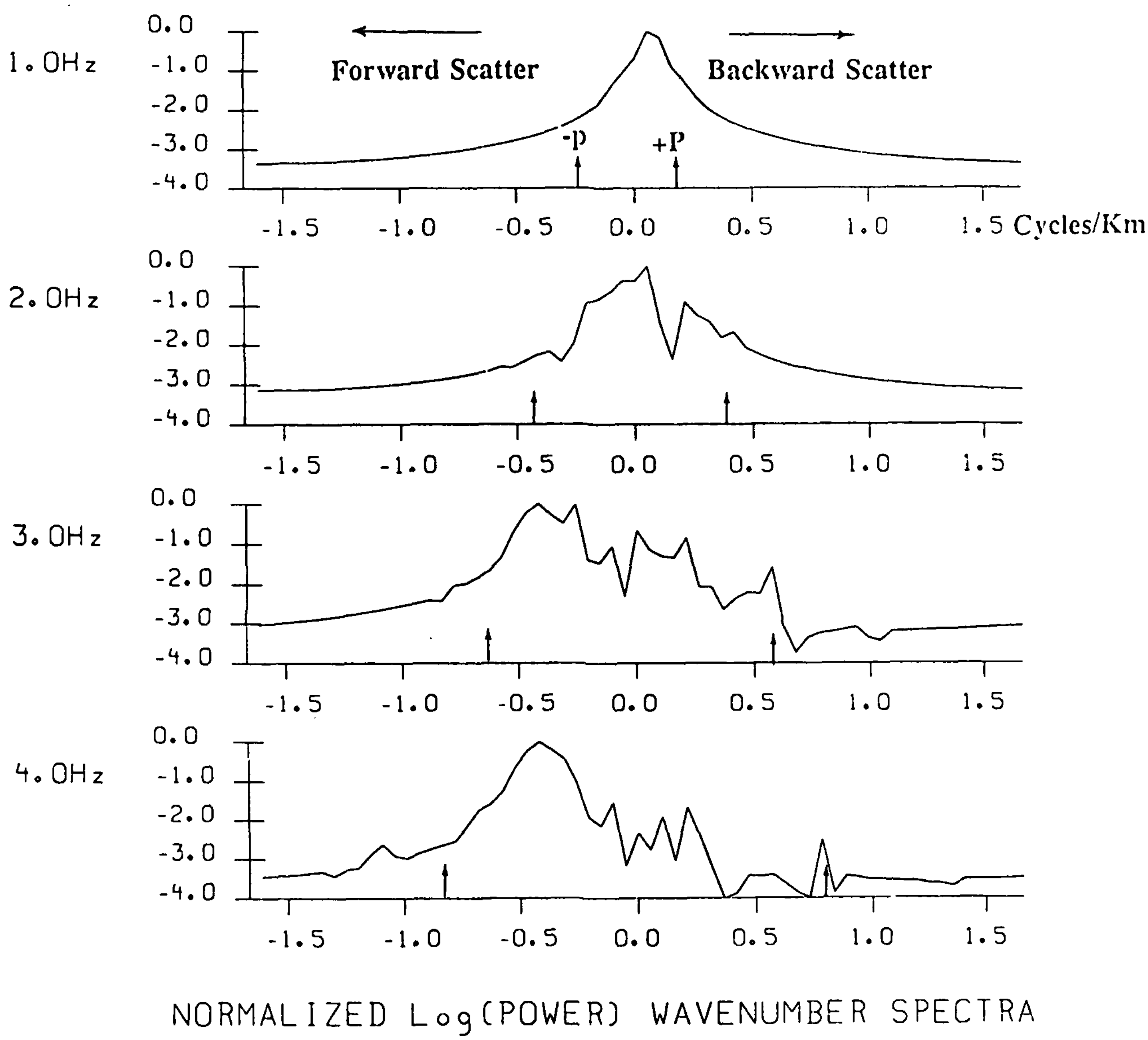

Figure 5.3 Frequency wavenumber spectra for the dilatational strain field (P-wave) recorded near the bottom of the grid with topography #5 on the top of the grid. The dilatational strain energy is largely confined to P wave slowness across the array. P wave energy shifts from back-scattered to forward-scattered from 1 to 4 Hz.

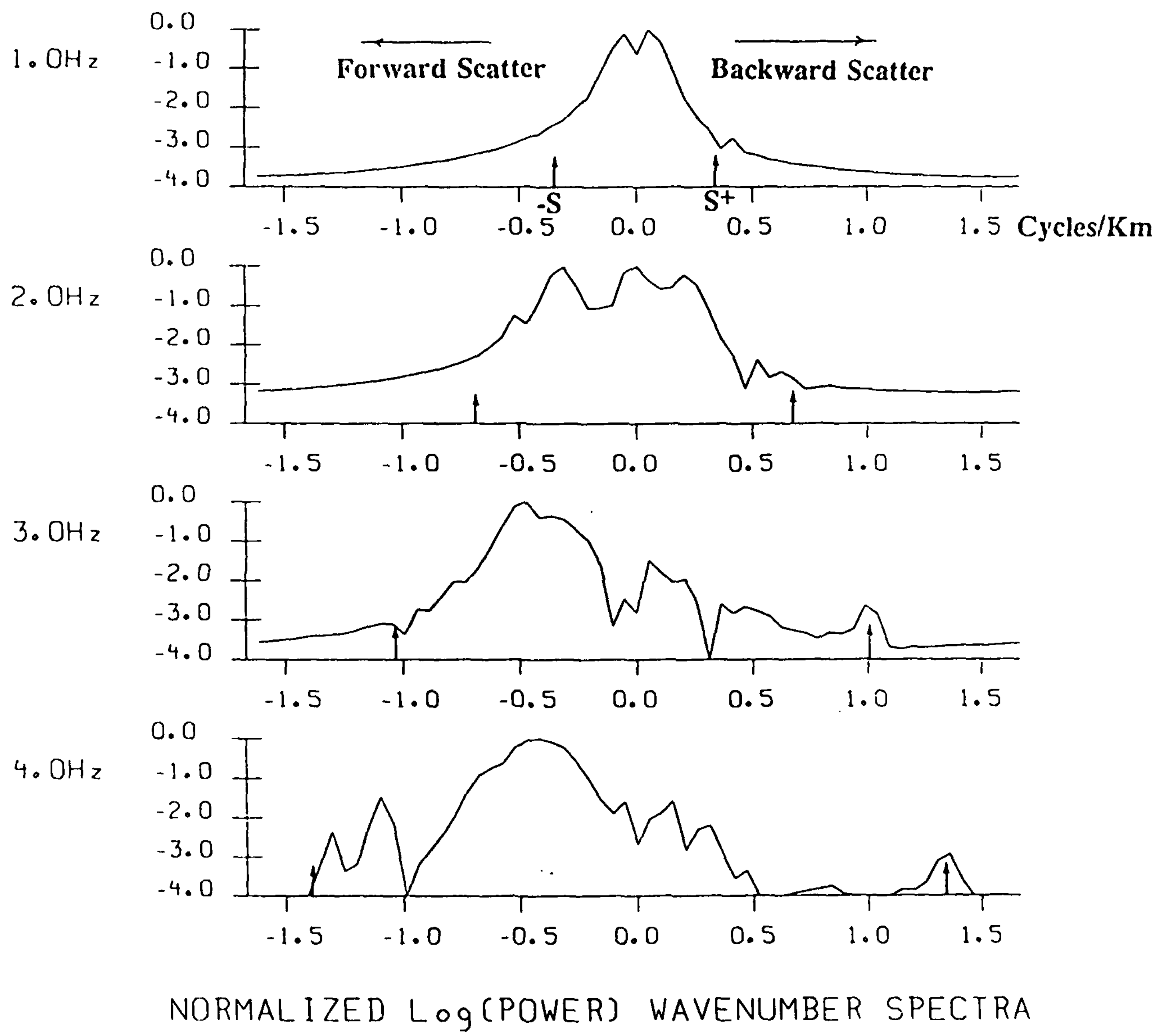

Figure 5.4 Frequency wavenumber spectra for the rotational strain field (S-wave) recorded near the bottom of the grid with topography #5 on the top. The rotational strain energy is largely confined to S wave slowness across the array. S wave energy shifts from back-scattered to forward-scattered from 1 to 4 Hz.

DISTRIBUTION LIST

Dr. Monem Abdel-Gawad
Rockwell International Science Center
1049 Camino Dos Rios
Thousand Oaks, CA 91360

Professor Keiiti Aki
Center for Earth Sciences
University of Southern California
University Park
Los Angeles, CA 90089-0741

Professor Shelton S. Alexander
Geosciences Department
403 Deike Building
The Pennsylvania State University
University Park, PA 16802

Professor Charles B. Archambeau
Cooperative Institute for Research in
Environmental Sciences
University of Colorado
Boulder, CO 80309

Dr. Thomas C. Bache Jr.
Science Applications Int'l Corp.
10210 Campus Point Drive
San Diego, CA 92121

Dr. James Bulau
Rockwell International Science Center
1049 Camino Dos Rios
P.O. Box 1085
Thousand Oaks, CA 91360

Dr. Douglas R. Baumgardt
Signal Analysis and Systems Division
ENSCO, Inc.
5400 Port Royal Road
Springfield, VA 22151-2388

Dr. S. Bratt
Science Applications Int'l Corp.
10210 Campus Point Drive
San Diego, CA 92121

Professor John Ebel
Department of Geology & Geophysics
Boston College
Chestnut Hill, MA 02167

Woodward-Clyde Consultants
Attn: Dr. Lawrence J. Burdick
Dr. Jeff Barker
P.O. Box 93245
Pasadena, CA 91109-3245 (2 copies)

Dr. Roy Burger
1221 Serry Rd.
Schenectady, NY 12309

Professor Robert W. Clayton
Seismological Laboratory
Division of Geological and Planetary
Sciences
California Institute of Technology
Pasadena, CA 91125

Dr. Vernon F. Cormier
Earth Resources Laboratory
Department of Earth, Atmospheric and
Planetary Sciences
Massachusetts Institute of Technology
42 Carleton Street
Cambridge, MA 02142

Professor Anton M. Dainty
Earth Resources Laboratory
Department of Earth, Atmospheric and
Planetary Sciences
Massachusetts Institute of Technology
42 Carleton Street
Cambridge, MA 02142

Dr. Zoltan A. Der
Teledyne Geotech
314 Montgomery Street
Alexandria, VA 22314

Prof. Adam Dziewonski
Hoffman Laboratory
Harvard University
20 Oxford St.
Cambridge, MA 02138

Professor John Ferguson
Center for Lithospheric Studies
The University of Texas at Dallas
P.O. Box 830688
Richardson, TX 75083-0688

Dr. Jeffrey W. Given
Sierra Geophysics
11255 Kirkland Way
Kirkland, WA 98033

Prof. Roy Greenfield
Geosciences Department
403 Deike Building
The Pennsylvania State University
University Park, PA 16802

Professor David G. Harkrider
Seismological Laboratory
Division of Geological and Planetary
Sciences
California Institute of Technology
Pasadena, CA 91125

Professor Donald V. Helmberger
Seismological Laboratory
Division of Geological and Planetary
Sciences
California Institute of Technology
Pasadena, CA 91125

Professor Eugene Herrin
Institute for the Study of Earth & Man
Geophysical Laboratory
Southern Methodist University
Dallas, TX 75275

Professor Robert B. Herrmann
Department of Earth and Atmospheric
Sciences
Saint Louis University
Saint Louis, MO 63156

Professor Lane R. Johnson
Seismographic Station
University of California
Berkeley, CA 94720

Professor Thomas H. Jordan
Department of Earth, Atmospheric and
Planetary Sciences
Massachusetts Institute of Technology
Cambridge, MA 02139

Dr. Alan Kafka
Department of Geology & Geophysics
Boston College
Chestnut Hill, MA 02167

Professor Charles A. Langston
Geosciences Department
403 Deike Building
The Pennsylvania State University
University Park, PA 16802

Professor Thorne Lay
Department of Geological Sciences
1006 C.C. Little Building
University of Michigan
Ann Arbor, MI 48109-1063

Dr. George R. Mellman
Sierra Geophysics
11255 Kirkland Way
Kirkland, WA 98033

Professor Brian J. Mitchell
Department of Earth and Atmospheric
Sciences
Saint Louis University
Saint Louis, MO 63156

Professor Thomas V. McEvilly
Seismographic Station
University of California
Berkeley, CA 94720

Dr. Keith L. McLaughlin
Teledyne Geotech
314 Montgomery Street
Alexandria, VA 22314

Professor Otto W. Nuttli
Department of Earth and Atmospheric
Sciences
Saint Louis University
Saint Louis, MO 63156

Professor Paul G. Richards
Lamont-Doherty Geological Observatory
of Columbia University
Palisades, NY 10964

Dr. Norton Rimer
S-Cubed
A Division of Maxwell Laboratory
P.O. 1620
La Jolla, CA 92038-1620

Professor Larry J. Ruff
Department of Geological Sciences
1006 C.C. Little Building
University of Michigan
Ann Arbor, MI 48109-1063

Professor Charles G. Sammis
Center for Earth Sciences
University of Southern California
University Park
Los Angeles, CA 90089-0741

Dr. David G. Simpson
Lamont-Doherty Geological Observatory
of Columbia University
Palisades, NY 10964

Dr. Jeffrey L. Stevens
S-CUBED,
A Division of Maxwell Laboratory
P.O. Box 1620
La Jolla, CA 92038-1620

Professor Brian Stump
Institute for the Study of Earth
and Man
Geophysical Laboratory
Southern Methodist University
Dallas, TX 75275

Professor Ta-liang Teng
Center for Earth Sciences
University of Southern California
University Park
Los Angeles, CA 90089-0741

Dr. R. B. Tittmann
Rockwell International Science Center
1049 Camino Dos Rios
P.O. Box 1085
Thousand Oaks, CA 91360

Professor M. Nafi Toksoz
Earth Resources Laboratory
Department of Earth, Atmospheric and
Planetary Sciences
Massachusetts Institute of Technology
42 Carleton Street
Cambridge, MA 02142

Professor Terry C. Wallace
Department of Geosciences
Building #11
University of Arizona
Tucson, AZ 85721

Prof. John H. Woodhouse
Hoffman Laboratory
Harvard University
20 Oxford St.
Cambridge, MA 02138

Dr. G. Blake
US Dept of Energy/DP 331
Forrestal Building
1000 Independence Ave.
Washington, D.C. 20585

Dr. Michel Bouchon
Universite Scientifique et
Medicale de Grenoble
Laboratoire de Geophysique
Interne et Tectonophysique
I.R.I.G.M.-B.P. 68
38402 St. Martin D'Heres
Cedex FRANCE

Dr. Hilmar Bungum
NTNF/NORSAR
P.O. Box 51
Norwegian Council of Science,
Industry and Research, NORSAR
N-2007 Kjeller, NORWAY

Dr. Alan Douglas
Ministry of Defense
Blacknest, Brimpton, Reading RG7-4RS
UNITED KINGDOM

Professor Peter Harjes
Institute for Geophysik
Rhur University
Bochum
P.O. Box 102148
4630 Bochum 1
FEDERAL REPUBLIC OF GERMANY

Dr. James Hannon
Lawrence Livermore National Laboratory
P.O. Box 808
Livermore, CA 94550

Dr. E. Husebye
NTNF/NORSAR
P.O. Box 51
N-2007 Kjeller, NORWAY

Dr. Arthur Lerner-Lam
Lamont-Doherty Geological Observatory
of Columbia University
Palisades, NY 10964

Mr. Peter Marshall
Procurement Executive
Ministry of Defense
Blacknest, Brimpton, Reading RG7-4RS
UNITED KINGDOM

Dr. B. Massinon
Societe Radiomana
27, Rue Claude Bernard
75005, Paris, FRANCE

Dr. Pierre Mechler
Societe Radiomana
27, Rue Claude Bernard
75005, Paris, FRANCE

Mr. Jack Murphy
S-CUBED
Reston Geophysics Office
11800 Sunrise Valley Drive
Suite 1212
Reston, VA 22091

Dr. Svein Mykkeltveit
NTNF/NORSAR
P.O. Box 51
N-2007 Kjeller, NORWAY

Dr. Carl Newton
Los Alamos National Laboratory
P.O. Box 1663
Mail Stop C 335, Group ESS3
Los Alamos, NM 87545

Dr. Peter Basham
Earth Physics Branch
Department of Energy and Mines
1 Observatory Crescent
Ottawa, Ontario
CANADA K1A OY3

Professor J. A. Orcutt
Geological Sciences Division
Univ. of California at San Diego
La Jolla, CA 92093

Dr. Frank F. Pilotte
Director of Geophysics
Headquarters Air Force Technical
Applications Center
Patrick AFB, Florida 32925-6001

Professor Keith Priestley
University of Nevada
Mackay School of Mines
Reno, Nevada 89557

Mr. Jack Raclin
USGS - Geology, Rm 3C136
Mail Stop 928 National Center
Reston, VA 22092

Dr. Frode Ringdal
NTNF/NORSAR
P.O. Box 51
N-2007 Kjeller, NORWAY

Dr. George H. Rothe
Chief, Research Division
Geophysics Directorate
Headquarters Air Force Technical
Applications Center
Patrick AFB, Florida 32925-6001

Dr. Alan S. Ryall, Jr.
Center for Seismic Studies
1300 North 17th Street
Suite 1450
Arlington, VA 22209-2308

Dr. Lawrence Turnbull
OSWR/NED
Central Intelligence Agency
CIA, Room 5G48
Washington, DC 20505

Professor Steven Grand
Department of Geology
245 Natural History Bldg
1301 West Green Street
Urbana, IL 61801

DARPA/PM
1400 Wilson Boulevard
Arlington, VA 22209

Defense Technical Information Center
Cameron Station
Alexandria, VA 22314 (12 copies)

Defense Intelligence Agency
Directorate for Scientific and
Technical Intelligence
Washington, D.C. 20301

Defense Nuclear Agency
Shock Physics Directorate/SS
Washington, D.C. 20305

Defense Nuclear Agency/SPSS
ATTN: Dr. Michael Shore
6801 Telegraph Road
Alexandria, VA 22310

AFOSR/NPG
ATTN: Director
Bldg 410, Room C222
Bolling AFB, Washington, D.C. 20332

AFTAC/CA (STINFO)
Patrick AFB, FL 32925-6001

AFWL/NTESC
Kirtland AFB, NM 87171

U.S. Arms Control & Disarmament Agency
ATTN: Mrs. M. Hoinkes
Div. of Multilateral Affairs, Rm 5499
Washington, D.C. 20451

U.S. Geological Survey
ATTN: Dr. T. Hanks
National Earthquake Research Center
345 Middlefield Road
Menlo Park, CA 94025

SRI International
333 Ravensworth Avenue
Menlo Park, CA 94025

Center for Seismic Studies
ATTN: Dr. C. Romney
1300 North 17th Street
Suite 1450
Arlington, VA 22209 (3 copies)

Dr. Robert Blandford
DARPA/GSD
1400 Wilson Boulevard
Arlington, VA 22209-2308

Ms. Ann Kerr
DARPA/GSD
1400 Wilson Boulevard
Arlington, VA 22209-2308

Dr. Ralph Alewine III
DARPA/GSD
1400 Wilson Boulevard
Arlington, VA 22209-2308

Mr. Edward Giller
Pacific Sierra Research Corp.
1401 Wilson Boulevard
Arlington, VA 22209

Science Horizons, Inc.
Attn: Dr. Bernard Minster
Dr. Theodore Cherry
710 Encinitas Blvd., Suite 101
Encinitas, CA 92024 (2 copies)

Dr. Jack Evernden
USGS - Earthquake Studies
345 Middlefield Road
Menlo Park, CA 94025

Dr. Lawrence Braile
Department of Geosciences
Purdue University
West Lafayette, IN 47907

Dr. G.A. Bollinger
Department of Geological Sciences
Virginia Polytechnical Institute
21044 Derring Hall
Blacksburg, VA 24061

Dr. L. Sykes
Lamont Doherty Geological Observatory
Columbia University
Palisades, NY 10964

Dr. S.W. Smith
Geophysics Program
University of Washington
Seattle, WA 98195

Dr. L. Timothy Long
School of Geophysical Sciences
Georgia Institute of Technology
Atlanta, GA 30332

Dr. N. Biswas
Geophysical Institute
University of Alaska
Fairbanks, AK 99701

Dr. Freeman Gilbert
Institute of Geophysics &
Planetary Physics
Univ. of California at San Diego
P.O. Box 109
La Jolla, CA 92037

Dr. Pradeep Talwani
Department of Geological Sciences
University of South Carolina
Columbia, SC 29208

University of Hawaii
Institute of Geophysics
Attn: Dr. Daniel Walker
Honolulu, HI 96822

Dr. Donald Forsyth
Department of Geological Sciences
Brown University
Providence, RI 02912

Dr. Jack Oliver
Department of Geology
Cornell University
Ithaca, NY 14850

Dr. Muawia Barazangi
Geological Sciences
Cornell University
Ithaca, NY 14853

Rondout Associates
Attn: Dr. George Sutton
Dr. Jerry Carter
Dr. Paul Pomeroy
P.O. Box 224
Stone Ridge, NY 12484 (3 copies)

Dr. M. Sorrells
Geotech/Teledyne
P.O. Box 28277
Dallas, TX 75228

Dr. Bob Smith
Department of Geophysics
University of Utah
1400 East 2nd South
Salt Lake City, UT 84112

Dr. Anthony Gangi
Texas A&M University
Department of Geophysics
College Station, TX 77843

Dr. Gregory B. Young
ENSCO, Inc.
5400 Port Royal Road
Springfield, CA 22151

Dr. Ben Menaheim
Weizman Institute of Science
Rehovot, ISRAEL 951729

Weidlinger Associates
Attn: Dr. Gregory Wojcik
620 Hansen Way, Suite 100
Palo Alto, CA 94304

Dr. Leon Knopoff
University of California
Institute of Geophysics & Planetary
Physics
Los Angeles, CA 90024

Dr. Kenneth H. Olsen
Los Alamos Scientific Laboratory
Post Office Box 1663
Los Alamos, NM 87545

Prof. Jon F. Claerbout
Prof. Amos Nur
Dept. of Geophysics
Stanford University
Stanford, CA 94305 (2 copies)

Dr. Robert Burridge
Schlumberger-Doll Research Ctr.
Old Quarry Road
Ridgefield, CT 06877

Dr. Eduard Berg
Institute of Geophysics
University of Hawaii
Honolulu, HI 96822

Dr. Robert Phinney
Dr. F.A. Dahlen
Dept. of Geological & Geophysical Sci.
Princeton University
Princeton, NJ 08540 (2 copies)

Dr. Kin-Yip Chun
Geophysics Division
Physics Department
University of Toronto
Ontario, CANADA M5S 1A7

New England Research, Inc.
Attn: Dr. Randolph Martin III
P.O. Box 857
Norwich, VT 05055

Sandia National Laboratory
Attn: Dr. H.B. Durham
Albuquerque, NM 87185

Dr. Gary McCartor
Mission Research Corp.
735 State Street
P. O. Drawer 719
Santa Barbara, CA 93102

Dr. W. H. K. Lee
USGS
Office of Earthquakes, Volcanoes,
& Engineering
Branch of Seismology
345 Middlefield Rd
Menlo Park, CA 94025

AFGL/XO
Hanscom AFB, MA 01731-5000

AFGL/LW
Hanscom AFB, MA 01731-5000

AFGL/SULL
Research Library
Hanscom AFB, MA 01731-5000 (2 copies)

Secretary of the Air Force (SAFRD)
Washington, DC 20330

Office of the Secretary Defense
DDR & E
Washington, DC 20330

HQ DNA
Attn: Technical Library
Washington, DC 20305

Director, Technical Information
DARPA
1400 Wilson Blvd.
Arlington, VA 22209

Los Alamos Scientific Laboratory
Attn: Report Library
Post Office Box 1663
Los Alamos, NM 87544

Dr. Thomas Weaver
Los Alamos Scientific Laboratory
Los Alamos, NM 87544

Dr. Al Florence
SRI International
333 Ravenswood Avenue
Menlo Park, CA 94025-3493

END
7-87
DTIC